A NUMERICAL INVESTIGATION ON THE AXIAL PULLOUT TESTS OF BURIED PIPES

by

Adeniyi Salami

A Thesis submitted to the

School of Graduate Studies

in partial fulfillment of the requirements for the degree of

Master of Engineering

Faculty of Engineering and Applied Science

Memorial University of Newfoundland

January 2022

St John’s Newfoundland

ABSTRACT

Pipelines may unavoidably be routed through areas susceptible to ground movement. The reliability of pipelines comes into question during events of ground movements due to generated loads due to ground movements. It is therefore imperative to accurately predict the loads generated to enable the proper design of pipelines. Many researchers have produced high-quality data from tests that idealize real-life conditions by pulling pipe through fixed soil, although in the actual event of ground movement, unstable soil moves away from stable soil that fixes the pipe. This study develops a finite element modeling technique to simulate laboratory conditions by pulling pipe through fixed soil, and the real-life condition is simulated by pulling soil while pipe is fixed in place. The finite element technique is also used to investigate the effect of pipe length, diameter, burial depth, and internal pressure for both steel and polyethylene pipes. The study reveals that short steel pipelines beginning from 1 m length developed a higher peak pull-out force for pipe pulling simulation compared to soil pulling simulation, this behaviour changes for longer steel pipelines from 6.5 m where soil pulling simulation predicts a higher peak pull-out force compared to pipe pulling simulation. Polyethylene pipelines simulated for pipe pulling predict higher peak pull-out forces of varying percentages with increase in length when compared to soil pulling. The effect of increase in soil width is not significant in the prediction of pull-out forces for both simulations. An increase in diameter and burial depth also increases pull-out forces for both simulations. Increase in pressure is not significant in the development of pull-out forces for steel pipelines while in polyethylene pipelines an increase in pressure increases development of pull-out forces.

ACKNOWLEDGEMENTS

The period of my master's program in the Faculty of Engineering and Applied Science at Memorial University of Newfoundland was very challenging due to the pandemic and other factors beyond my control but with the support of God and many individuals and agencies who stood by me I was able to complete my program. First, I would like to thank my supervisor, Dr Ashutosh Dhar who believed in me and gave me an opportunity to pursue my program. His guidance and mentorship proved very valuable throughout my study.

I also sincerely appreciate the School of Graduate studies, National Science and Engineering Research Council, Government of Newfoundland and Labrador, Fortis BC Inc., and WSP Canada who funded my research.

I appreciate Dr. Adebowale Oladepo and Dr Isaac Akinwumi who encouraged me to apply to MUN for further studies and provided valuable recommendations, encouragement, and moral support. I appreciate Dr. Lanre Sulaiman who continually encouraged me to push through and complete the program. I sincerely thank Auchib Reza, Parthebaan Murugathasan, and Cyprian Oton who provided technical knowledge and support throughout my study. I also appreciate all the laboratory attendants and technicians who were always available anytime I needed help

Lastly, I appreciate my wife Aderinsola, family and friends who provided emotional support and offered prayers to see that I complete my program.

Table of Contents

List of Figures

List of Tables

List of Symbols:

D = Diameter of the pipe

H = Buried depth from ground surface to the spring line of the pipe

L = Length of the pipe

$\gamma =$ Unit weight of soil

K_0 = Lateral earth pressure coefficient at rest

δ = Interface friction angle between pipe and soil

W_P = weight of the pipe

τ_f = shear stress at failure of the failure plain,

σ_f' = effective normal stress at failure of failure plane,

$\phi_m' =$ effective mobilized friction angle.

$\phi_m' =$ effective mobilized friction angle,

$\phi_c' =$ critical state friction angle,

$\Psi_m =$ dilation angle.

τ = shear stress,

c = cohesion,

σ = normal stress (negative in compression),

ϕ = angle of friction.

K = material constant

p_a = atmospheric pressure

p' = mean effective confining pressure

n = power function

E_s = Soil Young's Modulus

E_p = Pipe Young's Modulus

ν = Poisson's ratio

ρ = Density

CHAPTER ONE

INTRODUCTION

1.1 Background of Study

Pipelines are the most efficient and common means of transporting gas, water, sewage, and other fluids from one point to another. Cast iron, ductile iron, steel, and polymers are the most common types of pipe materials used for liquid, and gas transportation, and distribution systems.

Cast iron was the early pipe material that was replaced by ductile iron pipes starting in the early 1950s. Internal and external coatings are usually applied to the ductile and cast-iron pipes to protect them from corrosion (Kroon et al. 2004). Usage of ductile iron pipe is widespread in municipal water distribution systems.

In the last few decades, polyethylene pipe usage has increased due to its several advantages over metallic pipes, the most relevant being the cost. According to PIPA (2001), plastic pipes require less maintenance during their lifetime operation with proper design and installation techniques. Another key advantage is polyethylene has virtual freedom from the chemical attacks of soils and ambient water and moisture. Polyethylene is a non-conductor of electricity which makes it immune to corrosion induced by electrolytes such as salts, acids, and bases. Under external loading, plastic pipes offer greater deformation tolerance and stress relaxation. These advantages make plastic pipes preferable under challenging terrains.

Since geotechnical hazards can be a significant cause of damage to pipelines, the performance of buried pipeline systems in areas subjected to ground deformations is a significant engineering consideration. Landslides and earthquakes are examples of geohazards that cause relative ground movements and ground loads. The loads developed on a pipeline are a function of the direction of

ground movement and pipeline orientation. The direction of these ground movements can be either vertical, lateral, longitudinal, or any combination of these directions, as shown in Figure 1.1.

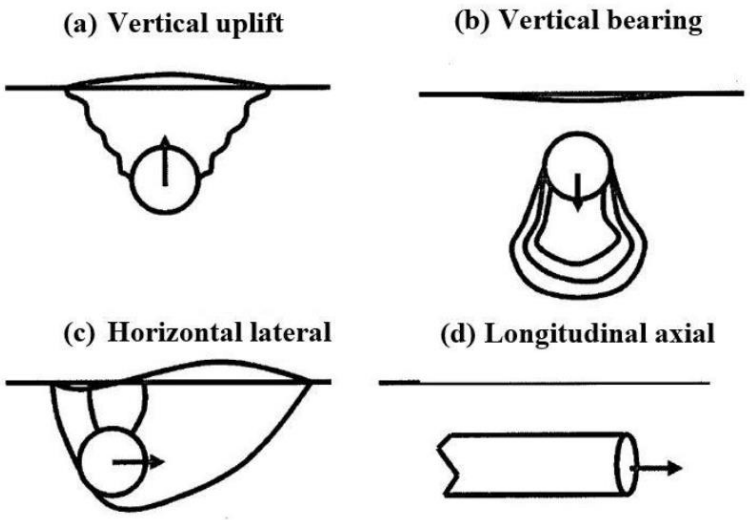

Figure 1.1 Anticipated mode of relative movement of pipe (Karimian, 2006)

External loads develop on the pipelines because of these relative ground movements. Figure 1.2 describes the schematics of pipelines subjected to ground loads (longitudinal and lateral) along their length during landslides. Pipes are subjected to axial or longitudinal loads when the pipe is parallel to the direction of ground movement and subjected to lateral load when the pipe is perpendicular to the direction of ground movement.

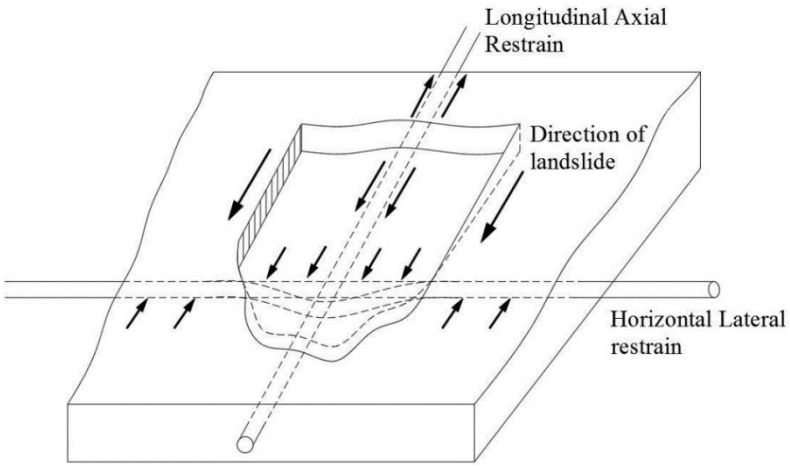

Figure 1.2 Pipeline subjected to axial and lateral ground movement (Karimian, 2006)

Where permanent ground deformation hazards are detected, major transmission pipelines are subjected to re-routing or re-alignment to avoid possible ground movement disruption. However, the placement of pipelines in areas prone to landslides is sometimes inevitable due to many reasons, such as geographical, environmental, and political factors. Remarkably, the municipal water distribution system and gas distribution system are needed in the community regardless of the community's exposure to geohazards. As a result, several design steps are considered during the design stage to ensure that pipelines are resistant to the geohazards.

1.2 Motivation of Study

When considering axial soil loading, the external load develops due to frictional resistance along the pipe. The primary design tool for pipelines subjected to axial soil loading has been the design equations recommended in ALA (2005) and PRCI (2009) guidelines that were adopted from ASCE (1984). In these guidelines, the pipeline is idealized as a structural beam, and soil-pipeline interaction is estimated using simple design equations applied to idealized conditions. Several experimental studies conducted to examine the applicability of this equation found that the equations are unsuccessful in predicting the maximum axial force on steel pipelines buried in dense

sand (Sheil et al. 2018; Wijewickreme et al. 2009). In the experimental studies, a pipe buried in a soil box was pulled with respect to a fixed soil mass. However, in a real-life scenario, an unstable soil mass moves while the buried pipe is fixed by the stable part of the ground, as shown in Figure 1.3.

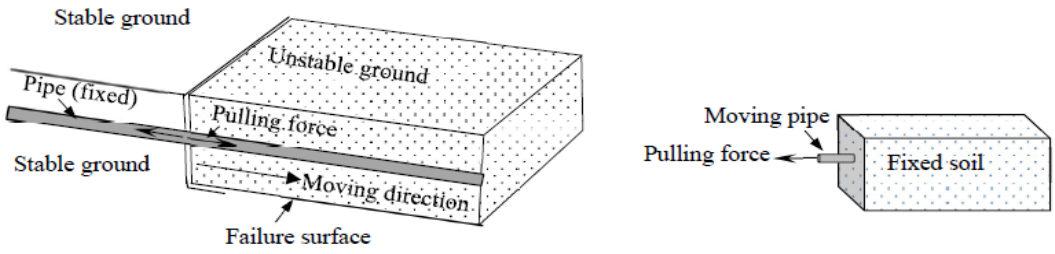

a) Field condition b) Laboratory idealization

Figure 1.3. Field and laboratory scenario of pipe subjected to ground movement (Murugathasan, 2019).

Therefore, it is essential to investigate if the idealized laboratory conditions provide the same axial pullout force as the conditions expected to occur in the field.

1.3 Objectives and Scope

The primary objectives of the thesis are:

- To examine the applicability of conventional test methods used for pipeline subjected to ground movement.
- To develop a numerical modeling technique for pulling pipes through a fixed ground and moving a soil mass against a pipe fixed at one end.

- To examine the effect of tests methods for steel and polyethylene pipes.

1.4 Framework of thesis

This thesis is developed in five chapters to present the findings of the study conducted.

Chapter 1 highlights the backgrounds, motivation, and objectives of the research.

Chapter 2 summarizes the literature related to the phenomenon of soil-pipeline interaction, permanent ground deformation, stress-strain behavior of backfill and finite element modeling techniques.

Chapter 3 presents the development of numerical models to simulate idealized laboratory and field conditions under different loading conditions.

Chapter 4 presents the results obtained from the numerical models and discusses the implications of such results for the pipeline industry

Chapter 5 presents the overall summary of the study with recommendations and suggestions for future research.

CHAPTER TWO

LITERATURE REVIEW

2.1 Introduction

Over the last few decades, many studies have been conducted to assess the buried pipelines' response to ground movement. These experiments include full-scale pipe pull-out tests, centrifuge tests, and field pipe tests. Several computational and analytical models were developed based on these experimental results to determine the response of buried pipes subjected to ground movements. This chapter presents a general overview of previous experimental and numerical studies reported on axial pipe-soil interaction behavior.

2.2 Pipe-soil interaction problem

Investigation of pipe-soil interaction to solve real-life problems can be at "element level" as well as "regional level". "Element level" refers to the analysis of the response of specific buried pipe configurations, whereas "Regional level" corresponds to the assessment of the vulnerability of a pipeline network subjected to regional ground movements.

In the "Element level" analysis, pipe-soil interaction is represented by a set of axial, lateral, and upward nonlinear soil springs. The development of these soil-spring models was based on model tests performed on steel pipes (Audibert and Nyman, 1977; Trautmann and O'Rourke, 1985, and Trautmann et al., 1985). Numerical analysis was also used to derive a solution for these pipe-soil interactions. The result obtained from these analyses was the basis of several guidelines such as 1) American lifeline Alliance (2001) "Guidelines for the design of buried steel pipelines, and 2) PRCI (2009), "Guidelines for seismic design and assessment of natural gas and liquid hydrocarbon pipelines".

"Regional level" analyses use fragility developed based on "Element level" analyses and apply those fragilities to a system of the pipeline through a GIS-based approach. The usefulness of this approach for vulnerability assessment of an existing gas transmission pipeline system has been described in Wijewickreme et al. (2005).

2.3 Soil load on pipeline

According to current guidelines (ASCE, 1984; ALA, 2001; PRCI, 2004), the axial soil resistance developed due to relative axial movement on straight pipes. For pipes buried in a cohesionless soil, the load can be calculated using Equation 2-1.

$$T_a = \gamma \pi D H L \frac{1+K_0}{2} tan\delta \qquad [2\text{-}1]$$

where,

D = Diameter of the pipe

H = Buried depth from ground surface to the spring line of the pipe

L = Length of the pipe

γ= Unit weight of soil

K_0 = Lateral earth pressure coefficient at rest

δ = Interface friction angle between pipe and soil.

This equation assumes an idealized soil pressure distribution around the pipe. Although the equation seems to be simple, the accuracy of the result is highly dependent upon the selection of the input parameters and the assumption used to develop Equations 2-1.

McAllister (2001) suggested including the weight of the pipe and proposed the following equation for determining the axial frictional resistance,

$$T_a = [2D\bar{\gamma}(H - \frac{D}{2}) + W_p]tan\delta \qquad [2\text{-}2]$$

where, W_P is the weight of the pipe which can be considered negligible for lightweight plastic pipes such as PE.

2.4 Studies on soil-pipe interaction

To understand the soil-pipe interaction for pipelines subjected to ground movement, various experimental and numerical studies were conducted. Some of these studies are discussed below.

2.4.1 Full-scale field testing

Experimental modeling pipe-soil interactions requires idealization of the soil mass movement with respect to the pipe. In a typical landslide, the soil mass is idealized with two zones: 1) Separation area at the top; 2) Soil accumulation area at the bottom of the slope (Figure 2-1). If the landslide occurs along the pipe axis, the sliding soil block will be separated from the stable ground in the separation zone thus creating tensile stresses in the pipe. The pipe is subjected to compression at the base of the landslide due to soil accumulation (Trigg and Rizkalla, 1994). According to Bughi et al. (1996), most slip failures would occur at a depth below 6 m in slow ground movements. Pipelines are typically buried at a depth of 0.3-1.5 m. Thus, the soil around the pipeline would be stable for slow moving ground unlike in rapid flows or liquefaction-induced ground movement. Most experimental studies focused on the slow-moving ground where the slide geometry is represented by two soil masses separating from each other as shown in Figure 2.1. It is, however, difficult to move a soil mass during the tests. As a result, a pipe is usually pulled relative to the soil to simulate the effects.

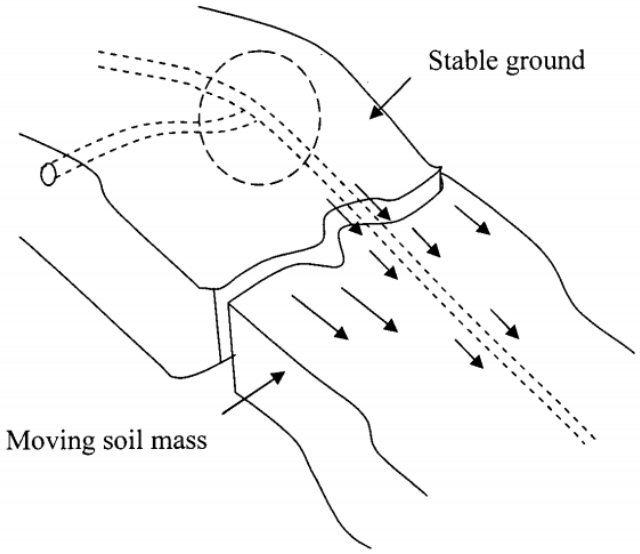

Figure 2.1: Landslide configuration (Weerasekara, 2007).

Field pull-out testing is valuable since the tests are conducted on pipe essentially under "real-life" conditions. However, literature on field pull-out tests is scarce because of the logistics required to carry out such tests. Audibert and Nyman (1977) performed a lateral pull-out test with a steel pipe of 230 mm diameter. Rizkalla et al. (1996) and Cappelletto et al. (1998) used a wide variety of backfill materials ranging from cohesionless soils to cohesive soils to perform the field axial pull-out test on buried steel pipes. They showed that current design recommendations for longitudinal pipe-soil interaction are overly conservative for cohesive soil backfill.

2.4.2 Full-scale laboratory testing

Laboratory test facilities are built with the idea that if burial depth and stiffness of the test wall facility is controlled same stress field can be simulated in the laboratory as would have occurred in the field (Murugathassan, 2019).

Trautmann and O'Rourke (1983, 1985) performed the first full-scale laboratory testing of soil-pipe interaction focusing on relative movements between pipe and soil at Cornell University. The

emphasis of these studies was on lateral and uplift loadings on steel pipelines in the sand, specifically the initial portion of the force-displacement response. These experiments used relatively quick displacements (20 mm/min) to model the effects of fault displacements on steel transmission pipelines. The researchers found that models adapted from vertical and strip anchors for computing maximum lateral soil forces were adequate for representing laboratory results. However, the study revealed an underestimation of projected loads for loose, contractive sands and that the maximum soil forces were nearly equal to those in dense sand for large ground movements, especially for lateral pipeline displacement.

Paulin et al. (1998) performed full-scale laboratory tests with steel pipes buried in the sand (loose and dense) and clay subjected to lateral and axial loadings. The maximum pulling capacity of the actuator used in these tests was 35-tonne and had a pulling rate capability of 0.5 to 10 mm/hr. The pulling rate of the pipe during the test was 10 mm/hr. According to the results of the experiments, the relative density of sand backfills had a significant impact on the mobilized soil resistance.

Wijewickreme et al. (2009) conducted full-scale laboratory tests using the testing facility at the University of British Columbia to investigate the behavior of buried steel pipes subjected to relative axial movement. They used the Fraser River sand as the backfill of buried pipe. The peak frictional angle of loose and dense sand was estimated as 43.5^0 and 45.5^0, respectively. Based on the direct shear test conducted in the laboratory, the interface friction angle measured for loose and dense sand were 33^0 and 36^0, respectively. The relative density, D_r, of the sand was maintained at 25% for loose sand and 75% for dense sand, respectively. In dense sand, the pipe burial depth was 2.5 times the diameter, and in loose sand, it was 2.7 times the diameter. The pulling rate of pipe ranged from 2 to 50 mm/s in a displacement-controlled manner. The study determined normal stress on the pipe using total pressure transducers. According to the results obtained from the

laboratory tests, ALA (2001) guideline underestimated the tests results regarding the maximum pull-out forces.

Bilgin and Stewart (2009) conducted extensive full-scale tests on cast iron pipes buried in sand to investigate the axial pipe-soil interaction. The outside diameter of the pipe used was 175 mm and the length was 3.66 m. The relative compaction of sand was 95%. The average dry unit weight and moisture content of dense backfill was 18.4 kN/m^3 and 5.3%, respectively. The burial depth used for the test was 0.76 m. The test result depicts that the peak soil resistance developed for dense fill was 10.4 kPa and for loose fill was 4.6 kPa. The authors proposed a simple model to estimate the interface shearing resistance in terms of constant cover depth, which was 6.0H, 9.3H, and 14H (H is the cover depth measure from the centre of pipe) for loose, medium, and dense sand, respectively, where the constant values depend on backfill soil properties.

Daiyan et al (2010) conducted a series of centrifuge tests to investigate the behavior of steel pipes buried in dense sand with a relative density of 82%. The inner dimension of the centrifuge model was 1180 mm × 940 mm × 400 mm. The diameter of the pipe used for the test was 41 mm with a length to diameter ratio of 8. The equivalent prototype length of the pipe was 504 mm, and the cover depth was 1008 mm. The average density of the sand was 1598 kg/m^3. The peak friction angle and the critical state friction angle were estimated using the direct shear test as 43^0, and 33^0, respectively. The centrifugal acceleration and displacement rate employed in the study were 9.3 g, and 0.04 m/s, respectively. The estimated friction coefficient at the pipe-soil interface was 0.44. The test result depicts that the axial interaction factor increases with pipe displacement up to 0.34 times pipe diameter. The investigation also showed that an axial interaction factor of 1.4 is needed to match the axial peak resistance while assuming the at-rest earth pressure coefficient.

Sheil et al. (2018) used a full-scale laboratory facility to test the buried steel pipe subjected to cyclic axial loads. The test cell construction employed 25-mm marine plywood panels with the internal dimensions of 1.83 m (depth) × 0.95 m (width) × 1.31 m (length). Two stiffened steel face panels with compressible foam seal around the pipe at the front and back end of the test cell ensured pipe settlement. The external diameter and thickness of the steel pipe used in the study were 350 mm and 6 mm, respectively. The pipe was divided into three parts to minimize the effects of the pull-out. The middle section was 500 mm long and connected to a separate load cell through a 'spindle' support system that ran through the inside of the pipe. The experiment used two types of sand (Houston HN31 and sand K). In the tests, the depth of soil cover ranged from 0.35 to 1.2 metres. Their findings showed that the axial resistance increased with the increasing overburden pressure during the first cycle. The soil resistance was higher for a narrow trench.

The results of the tests also demonstrated the importance of pipe weight and trench wall friction on mobilized soil loads. Due to the rigid inclusion effect, initial normal stress on the pipe crown was 20% higher than the nominal overburden pressure. The authors successfully predicted some test results using ALA's (2001) method when the at-rest lateral earth pressure coefficients (K_0) were assumed to be 0.5 and 1.0. However, some test results showed the ALA (2001) method's limitations. They suggested that pinching and trench effects cause inconsistencies between the test results and the prediction.

Murugathasan et al. (2019) investigated methods for predicting axial pull-out forces of buried pipes through an experimental program using the experimental test facility at Memorial University of Newfoundland. The backfill material employed for the test was a well-graded locally available sand with a coefficient of uniformity C_u = 5.8, coefficient of curvature C_c = 2.1, and moisture content of approximately 1%. Tekscan pressure sensors were placed to monitor the vertical and

horizontal earth pressures around the pipe. The study conducted five pull-out tests under various conditions, including different pipe burial depths, relative densities of soil, and pulling rates. The maximum pulling rate was 0.5 mm/sec and the slower rate was 0.017 mm/sec. The authors found from the investigation that the axial pull-out force is significantly affected by the relative density of soil. In dense sand, the maximum pull-out force was 1.3 times and 3.2 times higher than the pull-out force in medium dense and loose sand, respectively. Also, the unit interface shear resistance was 16.0H to 17.0H in dense sand, 13.0H in medium dense sand and 5.0H in loose sand where H is the cover depth measured from the center of the pipe. Reza and Dhar (2021) employed the facility at Memorial University to conduct the pull-out tests of Medium-density polyethylene pipe. They demonstrated that the pulling force for the pipe depends on the rate of displacement applied during axial pull-out.

2.4.3 Numerical studies

Various numerical studies, such as finite element methods, finite difference method, and discrete element method, were employed to investigate soil-pipeline interaction during the axial pullout of buried pipes. Among these, the finite element method is most used, which is discussed in more detail in the following section. Wijewickreme et al. (2009) employed an explicit finite difference approach using FLAC 2D to investigate the effect of soil dilation during shearing of interface soil. Instead of simulating the pull-out directly, the effect of soil dilation was mimicked by numerically widening the pipe (0.7 to 1 mm). The numerical model's typical stress increase was in good accordance with the experimental observation. Although a more robust numerical study would require a 3D simulation, a 2D simulation of the problem was adequate to simplify the problem’s solution.

Meideni et al. (2017) investigated the axial pipe-soil response of PVC pipes buried in granular material (Fraser River sand) using the discrete element method. The interface soil particle movement was successfully simulated using this approach. However, the successful application of this method depends on the proper choice of interaction parameters. Based on the analysis, Meideni et al. (2017) showed that during the axial pull-out, there was an increase in normal stresses around the pipe. They also observed much soil movement in the vicinity of the pipe, which eventually increased in the pull-out direction.

2.5 Finite element modeling

Many factors can affect pipe behavior like pipe material, surrounding soil material, installation procedure, loading conditions, time, and many others. Laboratory or field tests are limited to conducting exhaustive parametric studies to investigate failure modes as the tests are time-consuming and costly. In this case, a numerical simulation may be a practical alternative as it requires much less time and cost. The finite element approach is widely used in computer platforms to model complex engineering problems and find approximate solutions. Several standard computer software packages, such as Abaqus, ANSYS, and LS-Dyna, support the finite element process. The present study employed Abaqus for FE modelling. The following section considers some of the modelling features related to the pipe-soil interaction problem that are available in Abaqus.

2.5.1 Element types

Several solid element types in the Abaqus element library are suitable to model soil behaviour, such as C3D4, C3D8, C3D8R, and C3D20R. Almahakeri et al. (2016) successfully modelled soil behaviour using the C3D8R element, an eight-node linear brick element with hourglass control and reduced integration features. There are three active degrees of freedom in the C3D8R element.

The C3D20R element, a more flexible 20 node hexahedron element with a reduced integration function, was also used by the researchers. Almahakeri et al. (2016) stated that using this element in analyses caused convergence problems. Despite being a first-order element, this is a reduced integration element that prevents shear locking in the model.

2.5.2 Nonlinearities

The main sources of nonlinearity that can arise during the analysis of a model are material nonlinearity, geometric nonlinearity, and boundary conditions nonlinearity.

The geometric nonlinearity develops when a component experiences large deformation, which can cause the component to exhibit nonlinear behavior. The soil deformation close to the pipe is likely to be significant during the pipe pull-out. As a result, geometric nonlinearity is essential for consideration. The problem's geometric nonlinearity highlights the need for a nonlinear stiffness matrix. The features of geometric nonlinearity are available in Abaqus. It is important to set the time increment parameters correctly when geometric nonlinearity is present in the analysis.

The contact definition is an essential nonlinear boundary condition for the soil-pipe interaction problem. The interaction between two deformable bodies or a deformable body and a rigid body requires a contact definition. In this approach, the friction coefficient defines penalty-based tangential behavior (Coulomb friction model), which is dependent on the surface roughness.

When the stress-strain behavior of material shows non-linearity then it causes material nonlinearity. The pipe and the tank in this study are assumed to behave like elastic materials (to be discussed later in Chapter 3). However, the soil is an elastoplastic material that can reach a plastic state at low strain. This behavior of soil introduces material nonlinearity. Several models exist in Abaqus that can incorporate the plastic state of soil, such as Tresca, Von Mises, Drucker

Prager, and Mohr-Coulomb models. The Mohr-Coulomb model is widely used to model soil in previous research (Yimsiri et al. 2004; Guo and Stolle 2005; George et al. 2013; Almahakeri et al. 2016). The following section explores the details of Abaqus' built-in Mohr-Coulomb model.

2.5.3 Constitutive modeling of sand

2.5.3.1 Stress-strain behavior of sand

Sand's behavior is mainly affected by particle size distribution, grain sizes, natural gravity, and the angle of internal friction. The shear strength of sand is a function of the parameter related to interparticle friction (angle of internal friction and critical state friction angle) and volume change (dilation angle). The shear strength of sand can be represented by Equation 2-3 (here cohesion is assumed to be zero),

$$\tau_f = \sigma'_f \tan \phi'_m \qquad 2\text{-}3$$

where,

τ_f = shear stress at the failure of the failure plane,

σ'_f = effective normal stress at the failure of failure plane,

ϕ'_m = effective mobilized friction angle.

The mobilized angle of internal friction influences the dilation of dense sand (Rowe 1962; Mitchell 1963; Bolton 1986). Equation 2-4 (Bolton, 1986) estimates the peak angle of internal friction as a function of dilation.

$$\phi'_m = \phi'_c + 0.8\Psi_m \qquad 2\text{-}4$$

where,

ϕ'_m = effective mobilized friction angle,

ϕ'_c = critical state friction angle,

Ψ_m = maximum dilation angle.

Figure 2.2 shows the stress-displacement behavior of loose and dense sand in the triaxial condition. As the strain increases, the dense sand reaches a peak shear stress (measured as the deviatoric stress in the triaxial test) and then returns to a constant stress level, as shown in the figure. However, the loose sand does not peak; instead, it reaches a constant value when sheared to a significant strain level.

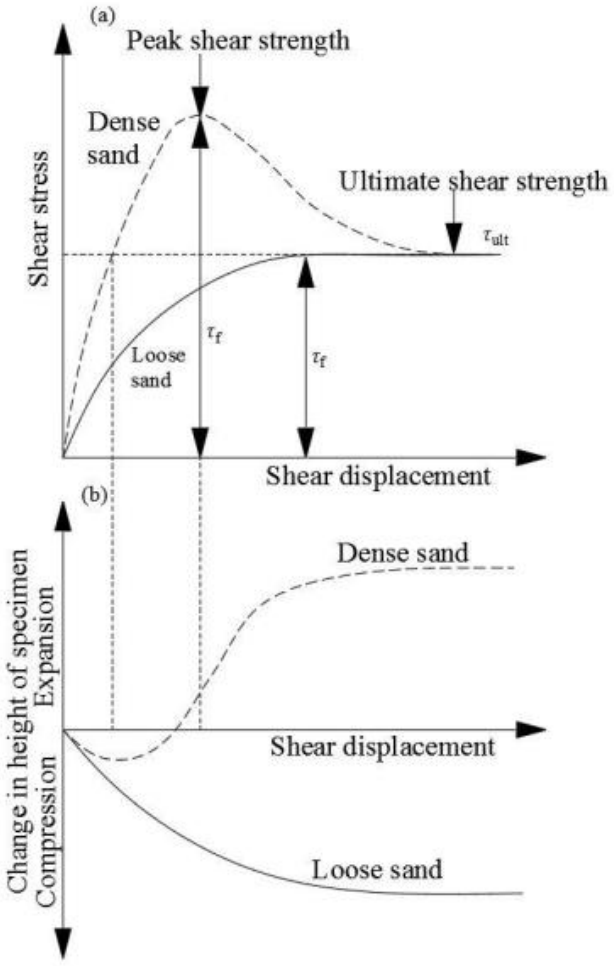

Figure 2.2: Typical drained triaxial test results of loose sand and dense sand: (a) Shear stress versus axial strain (b) Volumetric strain versus axial strain (Das 2008).

Figure 2.2(b) shows the relationship between volumetric strain and axial strain of soil. The expansion of soil is defined by the positive side of the vertical axis, while the negative side of the

vertical axis defines the contraction/compression of soil. The dense sand contracts initially, then expands until it reaches a constant volumetric strain, where the loose sand continuously contracts until it reaches a steady volumetric strain. The dilation angle is used to describe the gradient of this curve. The peak shear strength mobilizes when the dilation angle reaches its maximum value.

2.5.3.2 Mohr-Coulomb model

In finite element modelling, selecting an adequate soil constitutive model is critical for simulating the realistic sand behaviour. The Mohr-Coulomb failure criterion is one of Abaqus' built-in material models for simulating soil behaviour. In pipe-soil interaction problems, researchers successfully used the Mohr-Coulomb model to idealize the soil response (Yimsiri et al. 2004; Guo and Stolle 2005; Jung et al. 2013; Almahakeri et al. 2016).

The Mohr-Coulomb criterion assumes that the shear stress controls failure and that this failure shear stress depends on the normal stress. The shear stress can be represented by plotting Mohr's circle for stress levels at failure in terms of the maximum and minimum principal stresses (Figure 2-3). Thus, Equation 2.4 defines the Mohr-Coulomb criterion,

$$\tau_f = c' + \sigma'_f tan\phi'_m \qquad 2\text{-}5$$

where,

τ = shear stress at failure,

c' = effective cohesion,

σ'_f = effective stress at failure,

ϕ'_m = effective mobilized friction angle

According to this model, soil behaves like elastic-perfectly plastic where the soil behaves elastically until the stress state in the soil reaches the failure criteria.

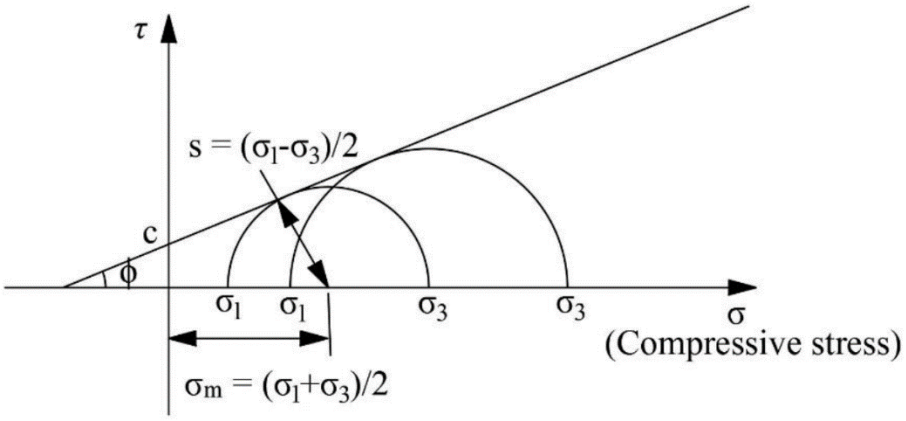

Figure 2.3: Mohr-coulomb failure criterion (Abaqus 2016)

Figure 2-4 shows the Mohr-Coulomb model in deviatoric plane. The friction angle (ϕ) controls the shape of the yield surface in the deviatoric plane. In the case of $\phi = 0°$, the Mohr-coulomb model reduces to the pressure-independent Tresca model with a perfectly hexagonal deviatoric section. Furthermore, when $\phi = 90°$, the Mohr-coulomb model reduces to the "tension cut-off" Rankine model with a triangular deviatoric section.

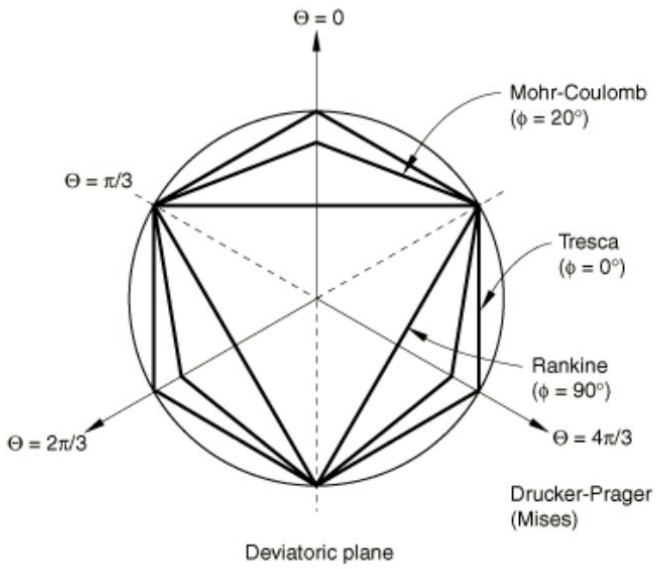

Figure 2.4: Mohr-coulomb yield surface in deviatoric planes (Abaqus 2016)

According to this model, as soil stresses hit the failure (yield) surface, plastic strains grow in the soil, and the soil dilates at a constant dilation angle. Since plastic strains grow in the soil even before it fails, and soil dilation is not constant, the behaviour of the soil varies slightly. However, during the pipe pull-out simulation, the MC model could be successfully used to estimate the ultimate soil resistance. Yimsiri et al. (2004) reported that the MC model provides a reasonable answer for the simulation of pipe-soil interaction.

2.6 Research needs from the literature review

This chapter provides an overview of current experimental and computational research on the axial pull-out of buried pipelines and different finite element modelling techniques for the pipe–soil interaction problem. The research and investigation need based on the literature review are summarized below:

- The laboratory idealization of axial pull-out test is based on relative movement of soil through the pulling of pipe. But in real field conditions, unstable soil moves away from stable soil while the pipe is restricted by the stable part of the soil. The difference in laboratory and field idealization necessitates comparing the pull-out forces generated in both conditions.
- The literature review shows that the experimental tests took place in experimental facilities of different dimensions. It is essential to find out whether the dimensions of experimental facilities influence the results of pull-out force.
- Liquids transportation through a pipeline occurs at a specific internal pressure. It is important to investigate the contribution of internal pressure to the development of axial pull-out force in buried pipelines subjected to axial ground movement. The effect of internal pressure was not investigated in the experimental studies available in the literature.
- Since the burial depth and pipe diameter plays a significant role in the development of axial pull-out force, it is imperative to investigate the effects of burial depth and pipe diameter on the development of axial pull-out force.

The scope of the current study is to focus on the research needs identified by developing numerical models using finite element software ABAQUS (version 6.14) to investigate the problem and make necessary recommendations from the results obtained.

CHAPTER THREE

FINITE ELEMENT MODEL DEVELOPMENT

3.1 Introduction

The finite element (FE) method is adopted to solve complex problems by approximating partial differential and integral mathematical equations. Obtaining the solution of the equations is achieved by discretizing the geometry of a structure into small parts called elements. Nodes interconnect the discretized elements which make up the geometry of the structure. Each element uses simple mathematical equations to approximate the response of the geometry at the location of the applied load. The addition of all the responses of the discretized elements contained in the domain provides the response of the domain to the applied load.

This study uses ABAQUS software to model the problem of a buried pipeline subjected to ground movement. The simulation performed considered the following assumptions:

- The pipeline is a continuous entity without any joints.
- Soil behaves following the Mohr-Coulomb theory, while the pipeline behavior is elastic.
- The interface between the soil-pipeline interface does not contain any defects.

Although the assumptions do not provide the exact conditions in real-life situations, they provide a reasonable basis to ensure the problem is simple to solve.

3.2 Three-Dimensional FE Model

For the finite element (FE) analysis, the soil and pipe were modeled as three dimensional (3D) deformable solid bodies. The performance of the FE simulation in simulating the soil-pipe interaction depends on the geometry of the model, mesh sizes, and material models used. Analysis

were performed with varying model geometry and mesh sizes to select these parameters. Fig 3.1 shows a typical FE the model geometry used in the analysis.

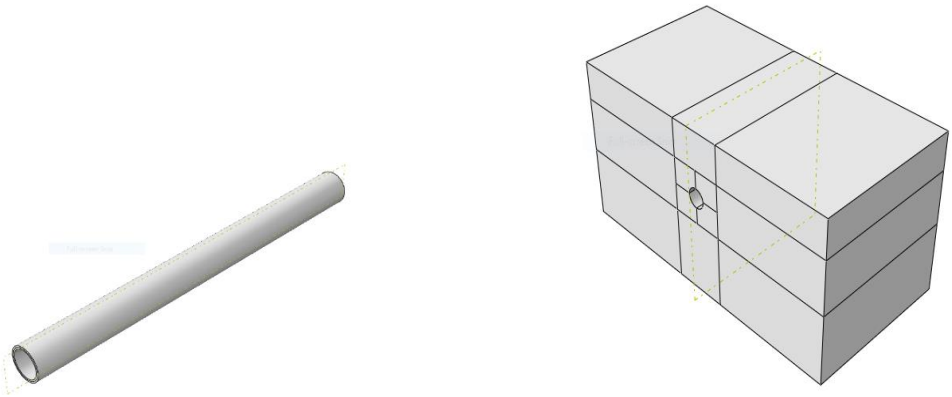

a) pipe b) soil mass

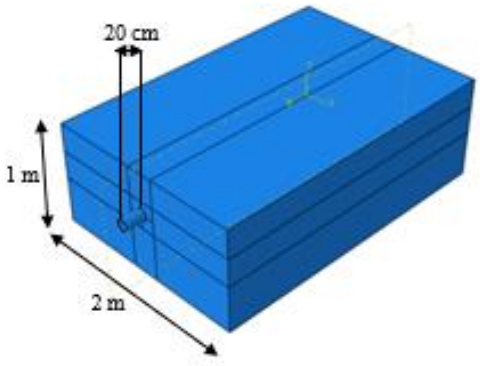

c) assembly

Fig 3.1 FE model geometry: a) pipe, b) soil mass, c) assembly

The pipe and soil mass are first defined with the desired geometry (Fig 3.1 a, b) and then assembled (Fig 3.1c). A contact area was established between the soil and the pipe to model the soil-pipe interface and create an assembly for the two materials to function as a structural unit. Several

models with different geometries were developed to investigate the effects. The pipe lengths considered include 1m, 3m, 6.5m and 9m buried at a depth of 400 mm in the soil.

Furthermore, to investigate the effect of burial depth, model width, and pipe diameter for different lengths of pipes, models of 1m and 6.5 m lengths were developed with different pipe diameters (60mm and 100mm diameters), different model widths (2m, 4m, and 6m) buried at 400 mm and 600 mm depths. The burial depth is 4 times the pipe diameter, representing deep burial scenarios. A total of 15 models were developed in this study as shown in Table 3.1

Table 3.1: Developed FE Models

Length (m)	Width (m)	Diameter (mm)	Depth (mm)	Total
1	2 4 6	60 100	400 600	6
2.7	2	178	825	1
3	2	60	400	1
6.5	2 4 6	60 100	400 600	6
9	2	60	400	1
				15

3.3 Material Models

In the present study, the materials used to model the problem are soil and the pipe (steel pipe or polyethylene pipe).

The soil was modeled as an elastoplastic material with Mohr-Coulomb plasticity. Typically, pipes are buried in dense sand because of the protection and the support dense sand offers. According to the Mohr-Coulomb plasticity theory, during the application of load on dense sand, expansion occurs when the material shears (at the yield surface), and plastic strains develop at a constant

dilation angle. There are some variations between the assumptions of Mohr-Coulomb theory and what occurs in the field where plastic strains can occur at a non-constant dilation angle. The Mohr-Coulomb theory is still useful for estimating the maximum soil resistance during axial pull-out (Muntakim and Dhar 2018). The parameters used to model dense sand in the current study are density (ρ), Young's Modulus (E), Poisson's ratio (ν), angle of internal friction (ϕ'), and dilation angle (ψ_m).

The magnitudes of the angle of internal friction and dilation angle for the dense sand were estimated based on available information in the literature (i.e., Saha et al. 2019). The angle of internal friction selected for the study was 40^0. The dilation selected for the study was 10^0 estimated from Bolton's equation (Equation 2.4). Although sand is a cohesionless material, for the purpose of achieving numerical stability, a small cohesion of 0.1 kPa was used. The Young's Modulus of the soil was estimated using Eq. (3.1) (Janbu 1963; Hardin and Black 1966)

$$E = Kp_a(\frac{p}{p_a})^n \qquad (3.1)$$

Where K is a material constant; p_a is the atmospheric pressure; p' is mean effective pressure; and n is a power function. For this study, the values of K and n are 150 and 0.5, respectively, following Roy et al. (2015). The Poisson's ratio of sand was assumed to be 0.3 in the analysis.

The pipe materials (steel and polyethylene) were assumed as linear elastic. The required material parameters for the pipes are density, Young's Modulus and Poisson's ratio.

The soil-pipe interface contact was modeled using the penalty contact algorithm available in the Abaqus software. The interface friction angle is a function of pipe surface roughness and the soil angle of interface friction δ (i.e., $\delta = f\phi$). In the present study, the pipe surface roughness was assumed to be 0.7. Tables 3.2 and 3.3 show the summary of the parameters used in the analysis.

Table 3.2: Pipe Parameters for FE Analysis

Parameter	Steel Pipe	Polyethylene Pipe
E_p (MPa)	200000	550
ν_P	0.3	0.46
ρ_P (kg/m^3)	7850	940
Pipe Diameter (mm)	60, 100	60, 100

Table 3.3: Soil Parameters for FE Analysis

Parameter	Steel Pipe	Polyethylene Pipe
E_S(MPa)	5	5
ν_S	0.3	0.3
$\boldsymbol{\phi'}$(°)	40	40
$\boldsymbol{\psi_m}$ (°)	10	10
ρ_S (kg/m^3)	1650	1650
Cohesion $\boldsymbol{c'}$ $(\boldsymbol{kN/m^2})$	0.1	0.1
Interface friction coefficient, $\boldsymbol{\mu}$	0.53	0.53
Burial depth (mm)	400, 600	400, 600

3.4 Boundary Conditions

The present study compares the scenario of pulling pipe through fixed soil and pulling soil with pipe fixed in place at one end. For the first condition of pulling pipe, the vertical boundaries (i.e., the left side, right side, front face, and back face of the soil geometry) of the FE model were fixed horizontally since the boundary walls are idealized as rigid. The bottom of the soil geometry was restrained in the horizontal and vertical directions. A displacement of 20 mm was applied to the leading end of the pipe. The pipe was extended beyond the boundary of the soil at the trailing end to ensure that the length of the pipe within the soil mass remains constant when the pipe is axially pulled (Figure 3.4a). In the second condition of soil movement with respect to the pipe, one end of the pipe is fixed (Figure 3.4b). The left side and right sides representing the walls of the soil geometry were fixed as the boundary walls in this condition are rigid. The bottom of the soil

geometry was restrained in the vertical direction (i.e., roller support). A 20 mm of displacement was applied to the soil nodes while fixing the leading end of the pipe.

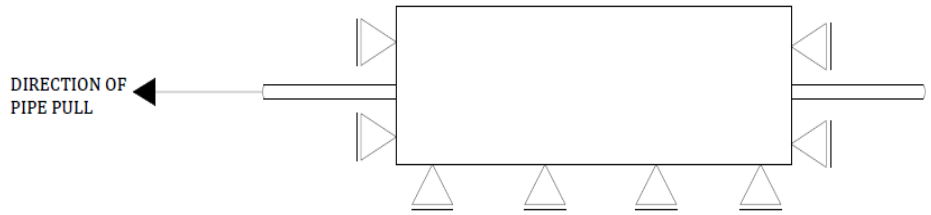

(a) Pipe pulling boundary conditions

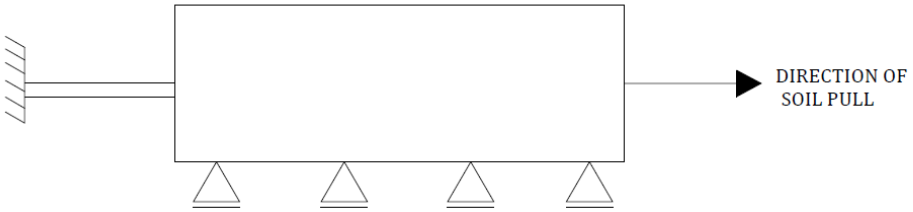

(b) Soil pulling boundary conditions

Fig. 3.4: Model boundary conditions

3.5 Mesh Discretization and Analysis Steps

The geometry of the soil and pipe was discretized using the eight-node linear brick element (C3D8R). To ensure the response of the soil-pipe interface is properly captured, a smaller mesh size was used in the soil geometry closer to the pipe, while larger mesh size was used away from

the pipe. A mesh sensitivity study was conducted, which predicts the smallest element size for the pipe to be 5 mm and the smallest element size for the soil to be 10 mm for the mesh type adopted in the study. Figure 3.5 shows the typical mesh adopted in the study. Figure 3.6 shows the results of a mesh sensitivity study carried out.

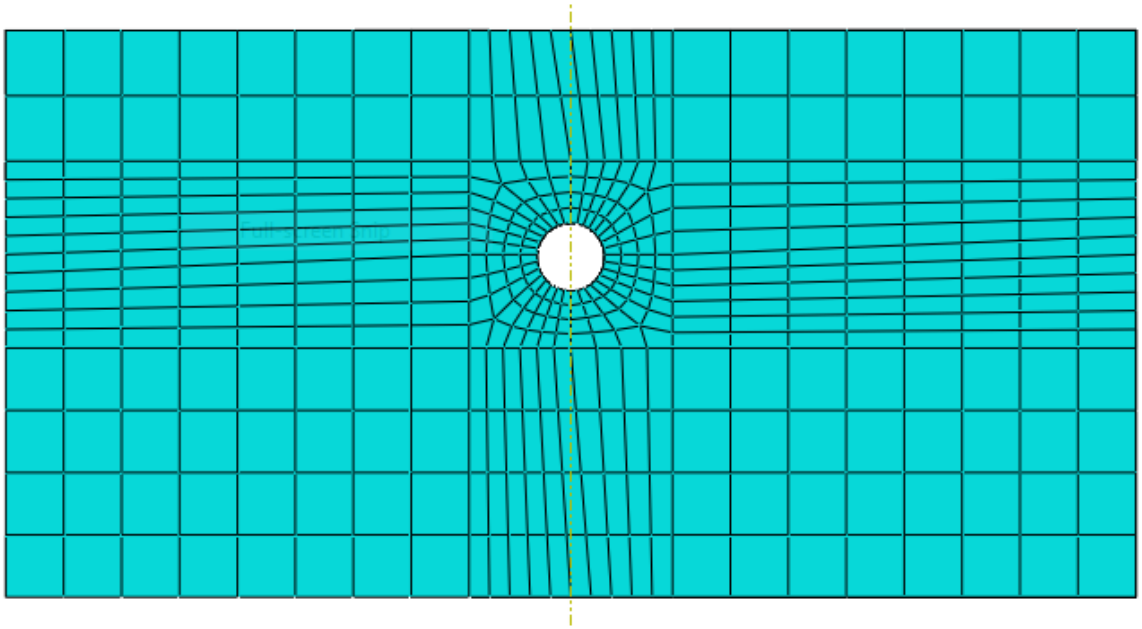

Fig. 3.5 Typical mesh adopted in FEA for all models

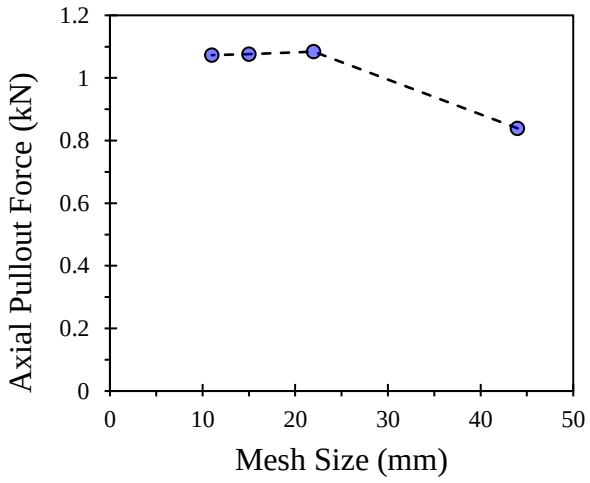

Fig. 3.6: Evidence of mesh sensitivity study

The analysis was conducted in 2 steps. In the first step, the self-weights of the soil and pipe were applied in 1 second to enable the generation of the initial stresses in the model. The second step was the pulling step. In this time step, the displacement of 20mm to the pipe (first scenario of pipe pull) or displacement of 20mm to the soil nodes (second scenario of soil pull) were applied in 1 second.

Analysis was also performed to examine the effect of internal pressure on axial pullout behavior. Internal pressures of 700 kPa and 2 MPa was applied, which are typical for water mains and gas distribution pipes, respectively. For this analysis, the self-weight was applied in the first step for 1 second, the internal pressure was applied in the second step for 1 second and the displacement of 20mm was applied in the following step (to the pipe in the first scenario of pipe pull and to the soil nodes in the second scenario of soil pull).

3.6 Model Validation

The model developed in the study was benchmarked using tests conducted by Murugathasan et al. (2019). A steel test pipe 2.7 m long was buried in dense sand at a depth of 825 mm in an

experimental tank and pulled axially at a rate of 0.5mm/sec. Figure 3.7 shows the comparison of pullout forces developed in the experiment and numerical analysis of pipe pull and soil pull. The peak pull-out force of both experimental data and pipe pull are comparable, which validates the model employed in this study. Note that the peak pull-out force for soil pull is less, implying that the mechanism of soil-pipe interaction is different during pipe pulling and soil pulling. The difference in soil-pipe interaction is discussed in Chapter 4.

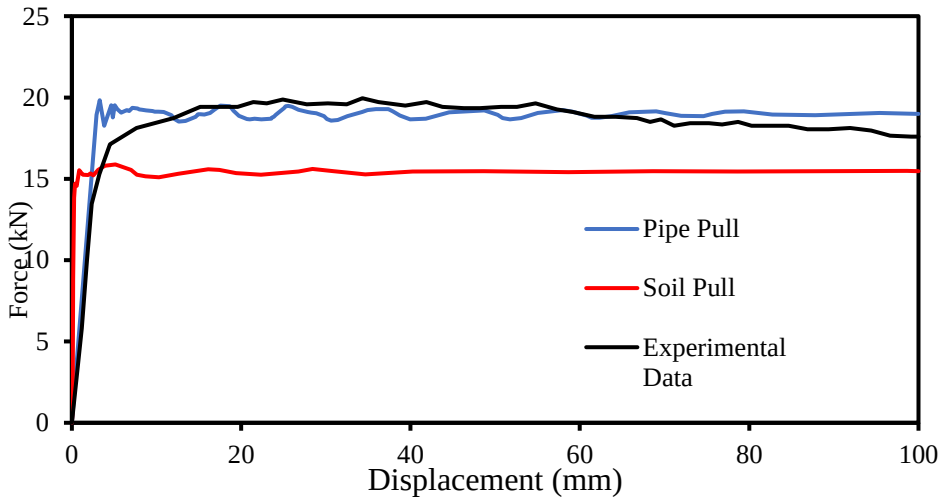

Fig 3.7: Model Validation

3.7 Summary

This chapter presents the research method employed to investigate the soil-pipe interaction. The present study involved the following steps:

- The soil and pipe were modeled as 3D deformable body.
- Finite element modeling techniques were used to investigate a scenario of pulling the pipe through a static soil mass and moving a soil mass against a static pipe. A displacement of 20 mm was considered sufficient to provide the maximum pulling force in each case.

- Finite element models were for various cases, including different pipe lengths (1 m, 3 m, 6.5 m, and 9 m), two different pipe diameters (60 mm and 100 mm) and two different burial depths (400mm and 600mm). Steel and polyethylene pipe materials were analyzed.
- A mesh sensitivity analysis was conducted which provided the smallest element (C3D8R) size requirement of 5 mm for the pipe, and the smallest element size 10-13 mm for the soil.
- Internal pressures (700 kPa and 2 MPa) were applied to simulate the operating conditions of water mains and gas distribution systems.

CHAPTER FOUR

RESULT AND DISCUSSION

4.1 Introduction

The discussion of results obtained in the study is presented in two sections; the first section presents the results obtained for the finite element analysis of steel pipelines, while the second section presents the results obtained for the finite element analysis of polyethylene pipes.

4.2 Investigation for Steel Pipes

In this study, the investigation for steel pipelines was conducted by modeling steel pipelines of various lengths (1 m, 3 m, 6.5 m, 9 m) and diameters (60 mm, 100 mm) buried at depths of 400 mm and 600 mm in soil. The effects of internal pressure on small diameter (60 mm) steel pipes were also investigated. An internal pressure of 700 kPa was applied to the pipe simulating a pipe transporting water while a pressure of 2 MPa was applied to the steel pipe to simulate a pipe transporting gas.

A comparison was made between pulling the pipe in the first instance to mimic the experimental conditions in the laboratory; in the second instance, the soil was pulled to mimic real-life conditions of ground movements where the soil moves. Presented in the section below are the results obtained from the various simulations.

4.2.1 Effect of pipe length on axial pull-out

The effect of length on small diameter pipe (60 mm) was investigated by considering four lengths 1 m, 3 m, 6.5 m, and 9 m. The result of axial pull-out was compared for both pulling of pipe and pulling of soil. Fig 4.1 shows the effects generated by increasing length of pipe buried at 400 mm depth.

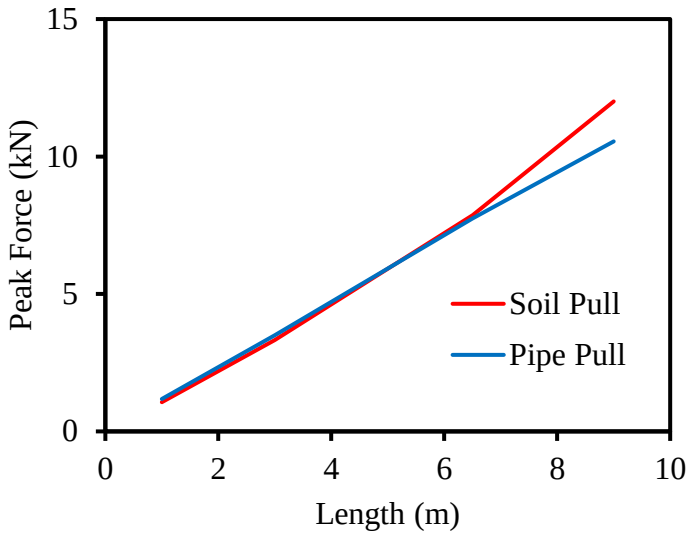

Fig 4.1: Effect of length on development of axial pull-out for steel pipe

From the results with an increase in length, there is a corresponding increase in axial pull-out force, which is due to increased frictional length in the model with increased pipe length. Figure 4.2 shows the percentage difference of peak pull-out force of pipe pulling simulation compared to soil pulling simulation.

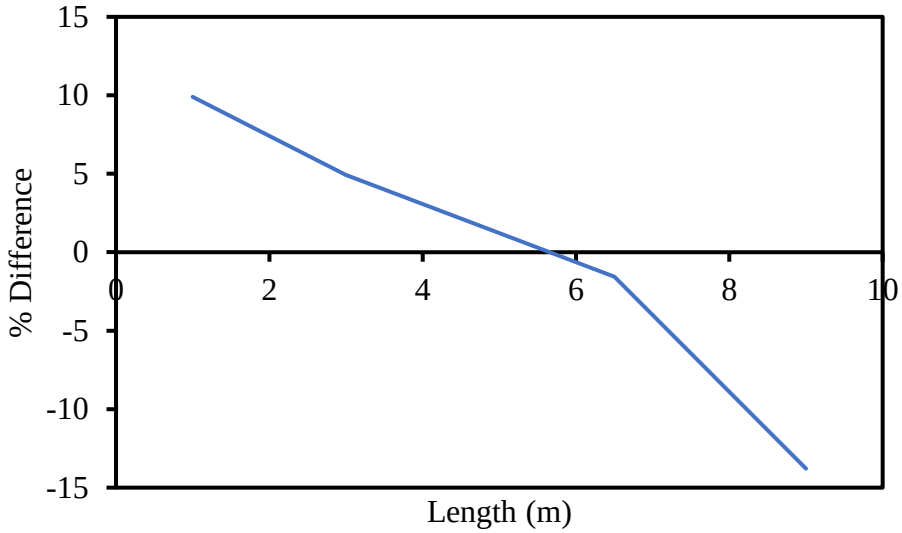

Fig. 4.2: Percentage difference of peak pull-out force for steel pipes

The result shows that for short steel pipes, the pipe pulling simulates higher peak pull-out forces than the soil pulling. However, for pipes longer than 6.5 m, the soil pulling predicts a higher pull-out force than those for pipe pulling.

To further gain insight into the effects of pipe pull and soil pull due to the increase in length of pipe, the results obtained for the 1 m and 6.5 m were carefully analyzed to understand the effect of length on axial pull-out. Figure 4.3 and Figure 4.4 show the comparison of the force-displacement relationship between soil pull and pipe pull for 1 m and 6.5 m length of pipe, respectively. The results show that the pulling force initially increases with the displacement until reaching a peak value. The pulling force is constant at the peak value at larger displacement when the frictional resistance of soil is fully mobilized over the entire length of the pipe. For 1 m long pipe, the peak pulling force for pipe pull is 9.9% higher than soil pull. However, for 6.5 m long pipe, the peak force for soil pull is 1.5% larger than for pipe pull. The difference might be due to the differences in load transfer mechanism for the pipe pull and soil pull cases for short and long pipes. For the case of pipe pull, pulling force is directly applied to the pipe, which is transferred along the pipe length gradually depending on the elongation of the pipe and the relative movement with respect to the surrounding soil. Thus, the axial stress along the pipe length may not be uniform. A similar phenomenon was observed for medium-density polyethylene pipe in Reza and Dhar (2021). However, for soil-pull tests, the relative displacement is applied uniformly over the entire pipe length at a time. As a result, axial stress along the pipe length is more likely to be uniform.

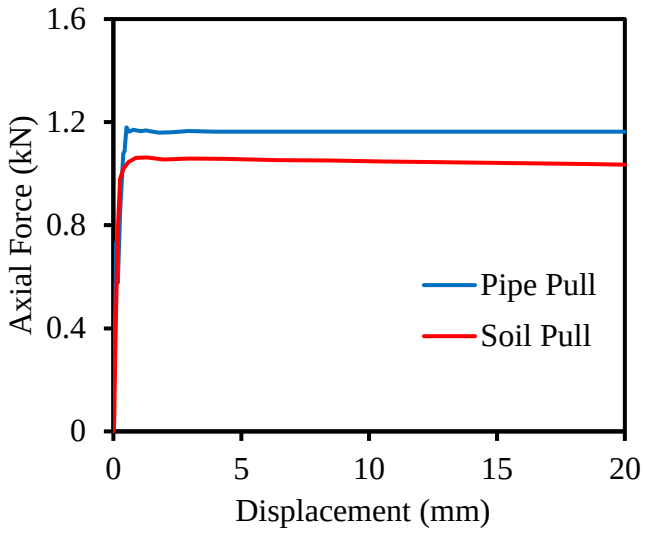

Fig. 4.3: Comparison of force-displacement relationship for 1 m steel pipe

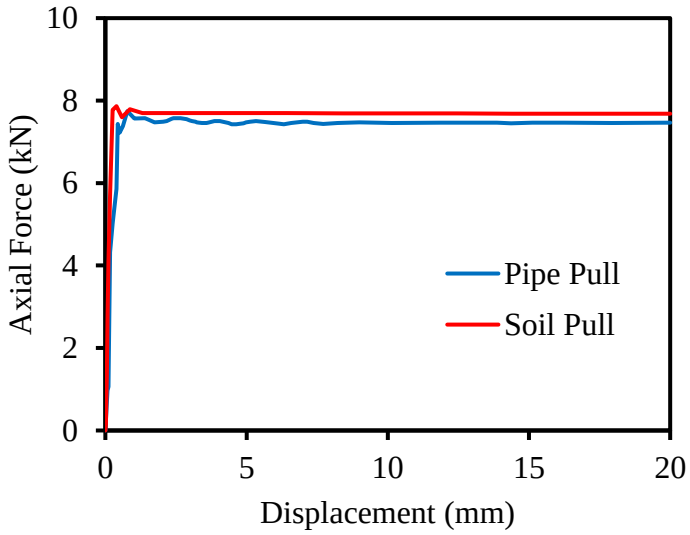

Fig. 4.4: Comparison of force-displacement relationship for 6.5 m steel pipe

To understand the load transfer mechanism, the axial stresses at different points along the pipe length are plotted in Figure 4.5 from the simulation with pipe pull and soil pull with the 6.5 m steel pipe.

The figure plots the axial stress at the pipe crown at a distance of L/4, L/2, and 3L/4 from the pipe pulling end and at corresponding points for soil pulling, where L is the length of pipe within the soil mass. In general, the stress is higher near the pulling end that reduces with distance from the leading end. Figure 4.5 shows that the axial stress mobilization along the pipe length is the different for the soil pull and pipe pull scenarios. The axial stresses are consistently tension along the pipeline during pipe pulling. However, the axial stress is compression towards the fixed end (i.e., ¼ length) and tension towards the other end (3/4 length) of the pipe during soil pulling. Due to the difference in the load transfer mechanisms, axial pull-out force can be different during pipe movement and soil movement. This aspect is not currently considered in the experimental design of pull-out testing of pipes.

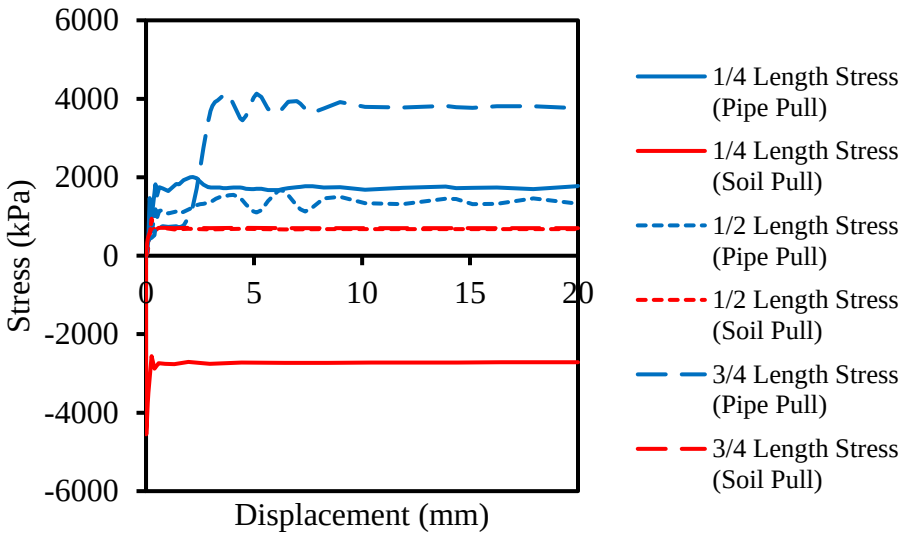

Fig. 4.5: Comparison of stress on 6.5 m pipe

The load transfer mechanism during pipe pulling and soil pulling might depend on the pipe and test cell geometry that as been investigated as discussed below.

4.2.2 Effect of soil width

Pipes of 1 m and 6.5 m lengths were investigated for varying soil widths of 2 m, 4 m, 6 m to examine the effect of width for any experimental facility on the pipe pull-out behavior. Figure 4.6 shows the effect of soil width on a 1 m steel pipe subjected to either soil pull or pipe pull. The results shows that pipe pulling simulation estimates a peak pull-out force about 10% higher than that for soil pulling simulation for the soil widths of 2 m and 4 m. A further increase in soil width to 6 m develops a comparable peak pull-out force for both pipe pulling and soil pulling simulations. Thus, the width of the test cell should be carefully considered for design of test facility.

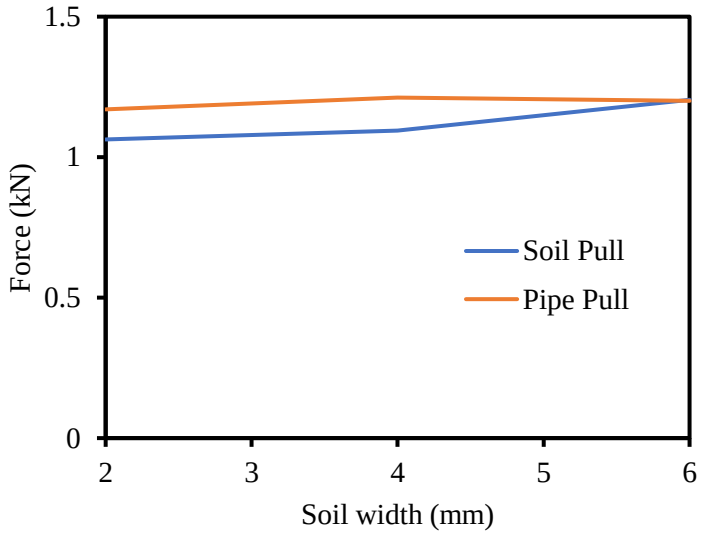

Fig. 4.6: Effect of soil width on 1 m steel pipe

Figure 4.7 shows the effect of soil width on a 6.5 m steel pipe subjected to either pipe pulling and soil pulling. Varying test cell width from 2 m to 6 m have significant effects on the simulations. The result for longer pipes shows comparable peak pull-out force irrespective of increasing soil width.

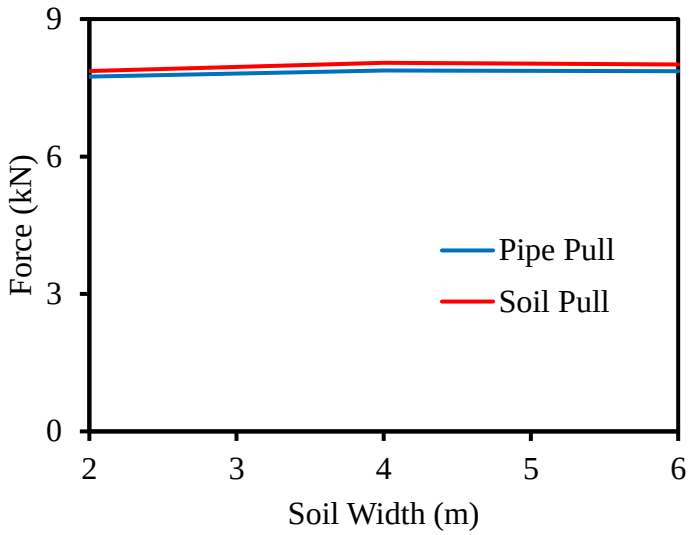

Fig. 4.7: Effect of soil width on 6.5 m steel pipe

4.2.3 Effect of pipe diameter

The study evaluated the contribution of pipeline diameter on axial pull-out behaviour by simulating steel pipes of 60 mm (small diameter) and 100 mm (large diameter) diameters buried at 400 mm depth.

Figure 4.8 shows the effect of diameter on the axial pull-out for 1 m length of pipe. A comparison of the results obtained for the soil pulling and pipe pulling for the modeled 1 m long steel pipe, as shown in Figure 4.8, predicts a 10% higher peak axial pull-out force for the pipe pulling when compared to the results of the soil pulling for 60 mm diameter steel pipe. Figure 4.8 also predicts a 27% higher axial pull-out force for the pipe pulling when compared to the results of the soil pulling for a 100 mm diameter steel pipe. The disparity between soil pulling and pipe pulling increases with an increase in pipe diameter, with the pipe pulling predicting a higher result as the diameter increases.

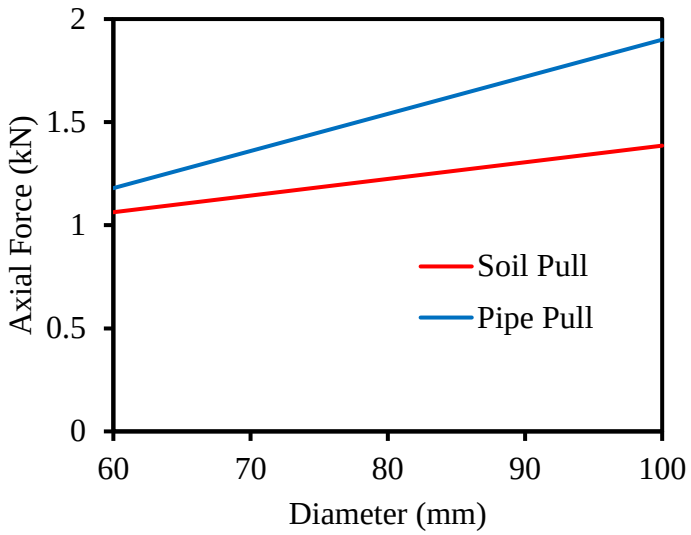

Fig. 4.8: Effect of pipe diameter for 1m steel pipe

Figure 4.9 shows the effect of diameter on the axial pull-out for 6.5 m length of pipe. The comparison of simulation of soil pulling and pipe pulling results for a 6.5m long steel pipe as shown in Figure 4.9 predicts that the results for pipe pulling and soil pulling are comparable for the 60 mm diameter pipe, an increase in the pipe diameter to 100 mm predicts that the soil pull results are 7.5% higher than the results obtained from the pipe pull.

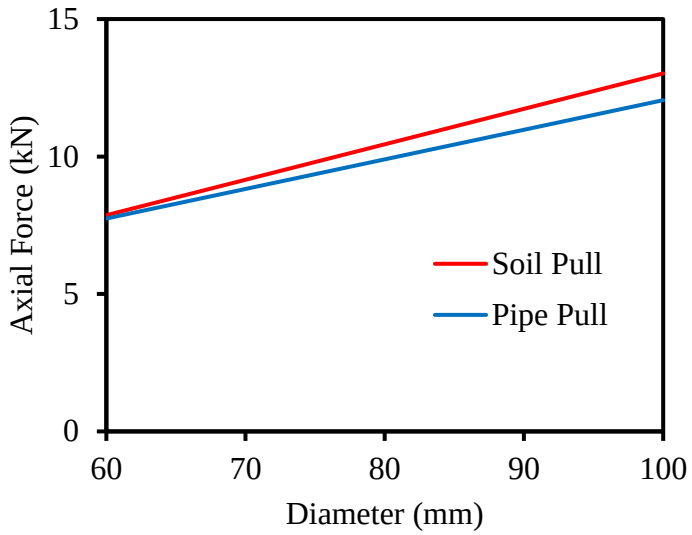

Fig. 4.10: Effect of pipe diameter for 6.5m steel pipe

The increase in peak pull-out force with increasing pipe diameter for both 1 m and 6.5 m pipes result from an increasing soil-pipe interface. An increased soil-pipe interface influences the frictional resistance between the soil and pipe, affecting the pipe's normal force.

The results of force and stress developed on the 100 mm diameter steel pipe of length 1m and 6.5m are shown in Figures 4.10 and 4.11. As mentioned earlier, a difference of 27% exists between the evaluated results of peak axial force for the pipe pulling and soil pulling in the simulation of the 1 m long, and 100 mm diameter pipe, this difference is vividly shown in Figure 4.10.

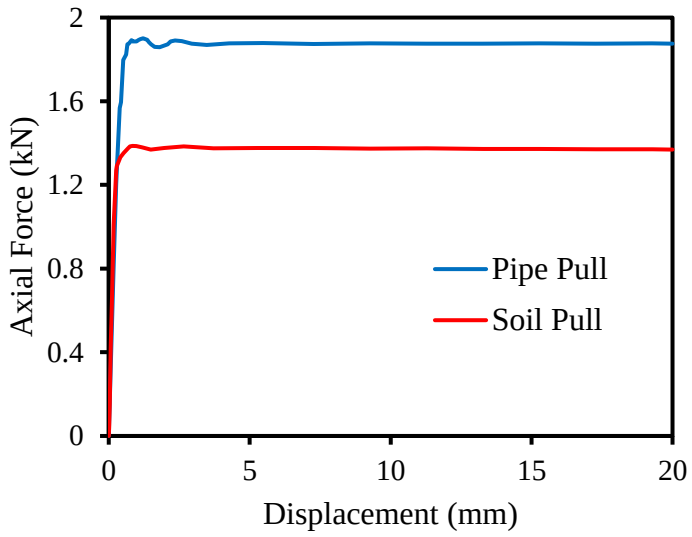

Fig. 4.10: Comparison of force-displacement relationship for 1m long, 100 mm diameter steel pipe

Figure 4.11 shows the comparison between the computed results of a 6.5 m long, 100 mm diameter pipe simulated for both soil pulling and pipe pulling. No significant difference in the axial force from pipe pulling and soil pulling in the figure in the stabilized zone (displacement > 5 mm shown in the figure). Note that some numerical instability was encountered during transition from the elastic responses to the elastoplastic responses. However, the maximum pulling force in the stabilized zone was not affected.

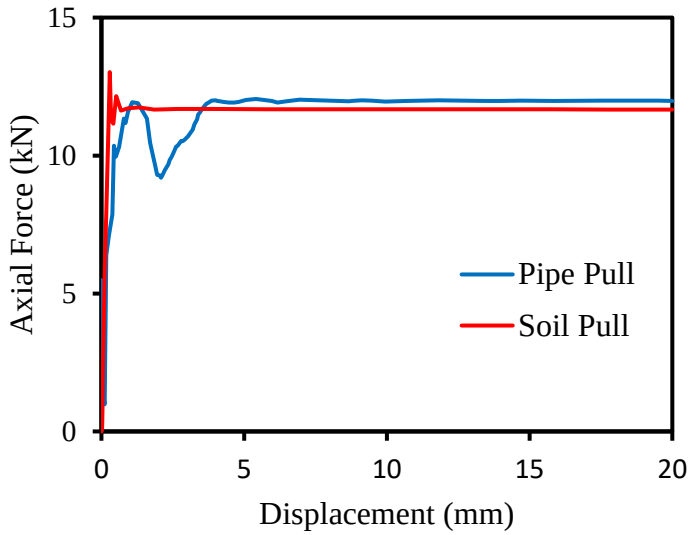

Fig. 4.11: Comparison of force-displacement relationship for a 6.5 m long, 100 mm diameter steel pipe

4.2.4 Effect of burial depth

The effect of burial depth was examined by simulating pipes of different lengths (1 m and 6.5 m) and different diameters (60 mm and 100 mm) buried at depths of 400 mm and 600 mm. Figure 4.12 and 4.13 shows the FEA results. There is a consistent increase in axial pull-out force with an increase in burial depth, which is due to an increase in soil overburden pressure on the pipe. The effect of burial depth on the pulling force due to pipe pull and soil pull is not very significant as shown in Figure 4.12 and 4.13. For the 1 m pipe, the pulling force versus burial depth responses from the two methods of loading are almost parallel to each other for 100 mm diameter pipe. For all other cases, the responses are close to each other.

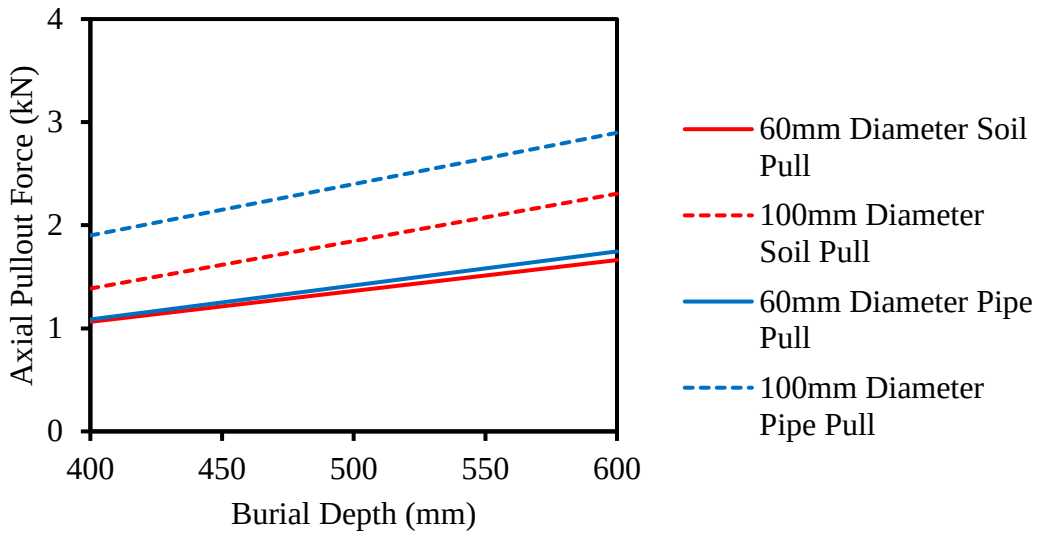

Fig. 4.12: Effect of burial depth on 1m long steel pipe

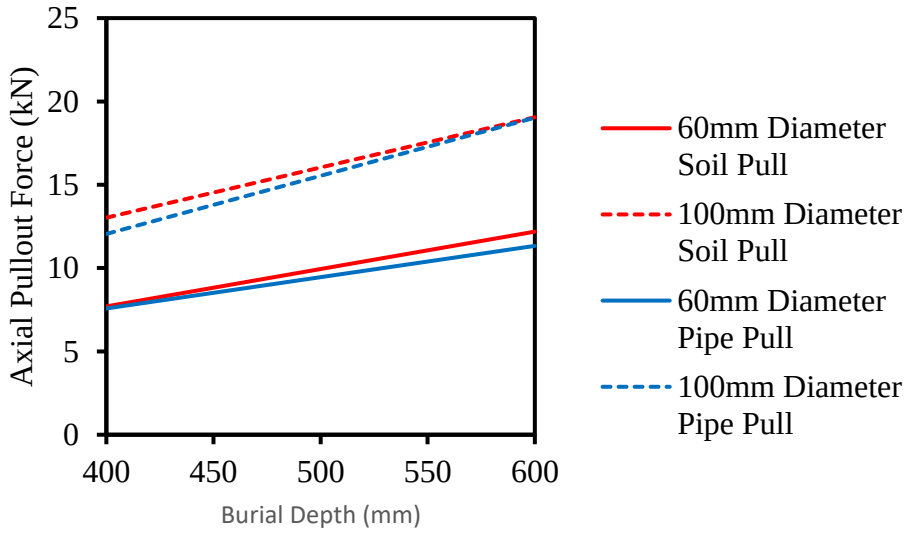

Fig. 4.13: Effect of burial depth on 6.5m long steel pipe

4.2.5 Effect of internal pressure

In most pipe-soil interaction available in published literature, the effect of internal pressure is usually neglected. However, pipes in service carry liquid or gas at the design pressures. The common design pressures for water pipes and gas pipes are 700 kPa and 2 MPa, respectively.

This study investigated the effect of internal pressure on steel pipes subjected to axial ground movement. A pressure of 700 kPa simulated water transportation through the 60 mm steel pipe diameter buried at a depth of 400 mm, while a pressure of 2 MPa simulated gas transportation through the 60 mm steel pipe diameter buried at a depth of 400 mm. Figure 4.14 and 4.15 shows the force-displacement diagram for a 1 m and 6.5 m long steel pipe, respectively. The figure compares soil pulling and pipe pulling for no internal pressure case and internal pressure case.

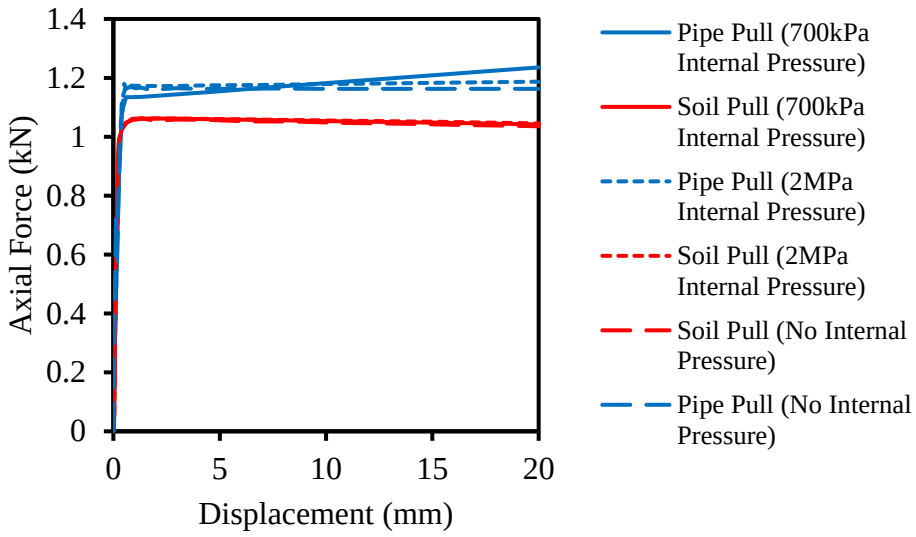

Fig 4.14: Effect of internal pressure on a 1m long, 60mm diameter steel pipe

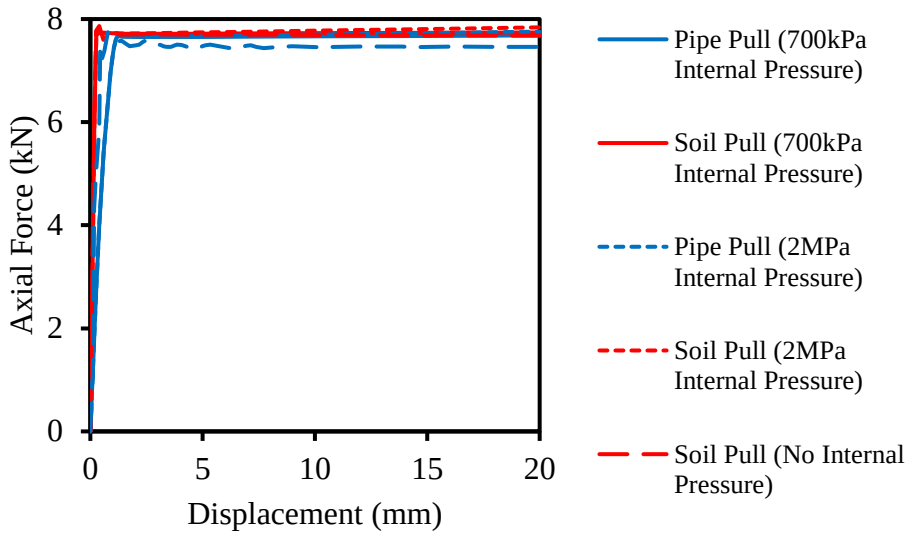

Fig. 4.15: Effect of internal pressure on 6.5m long, 60mm diameter steel pipe

From the figures, internal pressure in steel pipes appears to have no significant effect in the development of axial pull-out force when they are subjected to axial ground movement. The maximum pull-out force for the condition without pressure is comparable to the maximum pull-out force generated for the conditions with pressure. This may be because the change in diameter due to internal pressure is negligible for steel pipes. Therefore, the behavior of the steel pipes for conditions with pressure can be investigated as the conditions without internal pressure.

4.3 Investigation for Polyethylene Pipes

In this study, the investigation for polyethylene pipes was conducted by modelling polyethylene pipelines of various lengths (1 m, 3 m, 6.5 m, 9 m) and diameter (60 mm, 100 mm) buried at depths of 400 mm and 600 mm in modeled soil. The effects of internal pressure on small diameter (60 mm) polyethylene pipes were also investigated. A pressure of 700 kPa was applied to the pipe simulating a pipe transporting water, while a pressure of 2 MPa was applied to the steel pipe to simulate a pipe transporting gas.

A comparison was made between pulling the pipe in the first instance to mimic the experimental conditions usually used in the laboratory tests (i.e., Reza and Dhar, 2021). In the second instance, the soil was pulled to mimic real-life conditions of ground movements where the soil moves. Presented in the section below are the results obtained from the various simulations.

4.3.1 Effect of pipe length

The effect of length on small diameter pipe (60 mm) was investigated by considering four lengths, 1 m, 3 m, 6.5 m, and 9 m. The result of axial pull-out was compared for both pulling of pipe and pulling of soil. Figure 4.16 shows the effects generated by increasing length of pipe buried at 400 mm depth. It can be observed from the figure that there is a consistent increase in peak pull-out force with an increase in length, which is attributed to the increase in frictional length as the pipe length increases. Similar behaviour was also observed in steel pipes. However, the responses are more nonlinear for the polyethylene pipes. The nonlinear force-displacement responses of the polyethylene pipes are associated with large deformation of the pipe due to the lower modulus of elasticity of the pipe material.

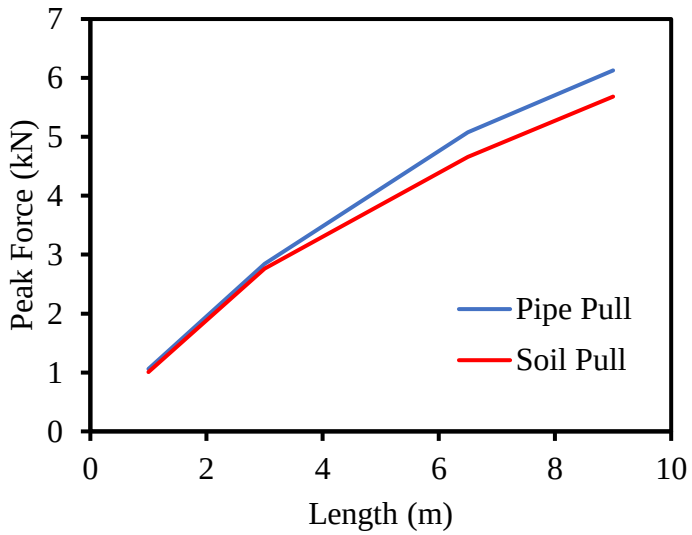

Fig. 4.16: Effect of length on the development of axial pull out for polyethylene pipe

Figure 4.16 also reveals that the peak pull-out force from soil pull is different depending on the pipe samples length.

Figure 4.17 shows the percentage difference between the results of pipe pull simulation and soil pull simulation. The result shows that peak forces predicted by pipe pull simulations are higher than peak forces predicted by soil pull simulation, regardless of the pipe length. However, the percentage increase varies with the increase in length of pipe. Note that, for steel pipes, the forces from the pipe pull were greater for shorter samples and smaller for longer samples than the forces from soil pull.

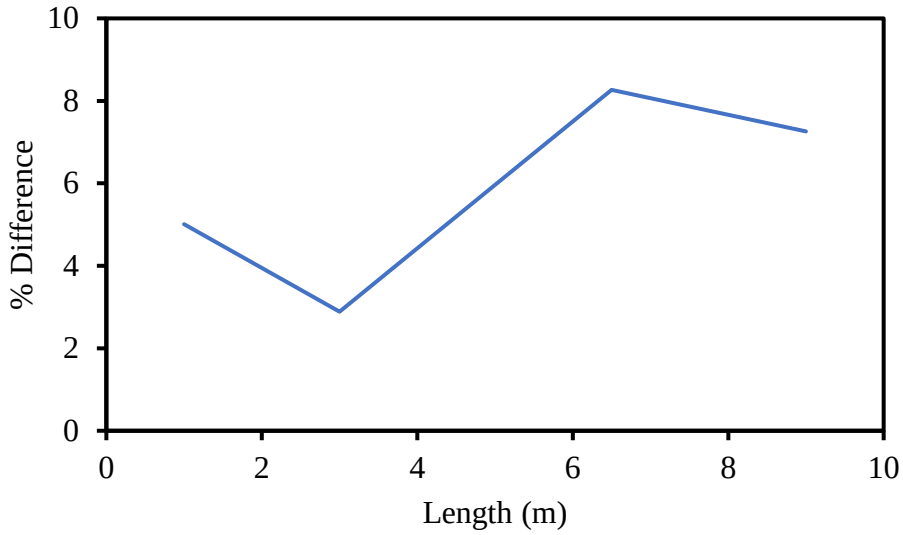

Fig. 28: Percentage difference between pipe pull and soil pull for polyethylene pipe

An insight can be gained into this behaviour by examining the pull-out behavior of a shorter pipe sample (1 m) and a longer pipe sample (6.5 m). The results of both pipes are discussed below.

The comparison of force-displacement results for the 1 m pipe is shown in Figure 4.18. In this figure, the pipe pulling results are comparable with the soil pulling results.

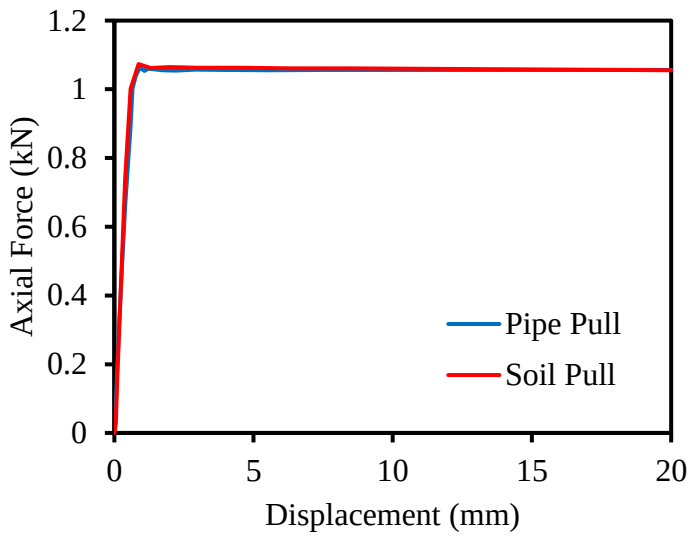

Fig. 4.18: Comparison of force-displacement relationship for a 1m polyethylene pipe

For polyethylene pipes, the effect of pipe wall strains is expected to be significant due to relative ground movement. The pipe axial strains obtained from the simulations at various points along the length are plotted in Figure 4.19. The strain results were obtained at distances of L/4, L/2, and 3L/4 (as before). It shows that even though the maximum pull-out forces are comparable from simulations using pipe pull and soil pull, there differences in calculated strain. At L/4, the pipe generated tensile strains, which are the highest amount of tensile strain in the entire length of pipe for both pipe pulling and soil pulling simulations but the magnitude of strain at L/4 for pipe pulling is higher than the magnitude strain for the soil pulling. Thus, the load transfer mechanism to the pipe is different for pipe pulling and soil pulling. The difference between the calculated strains reduces with the distance from the leading end.

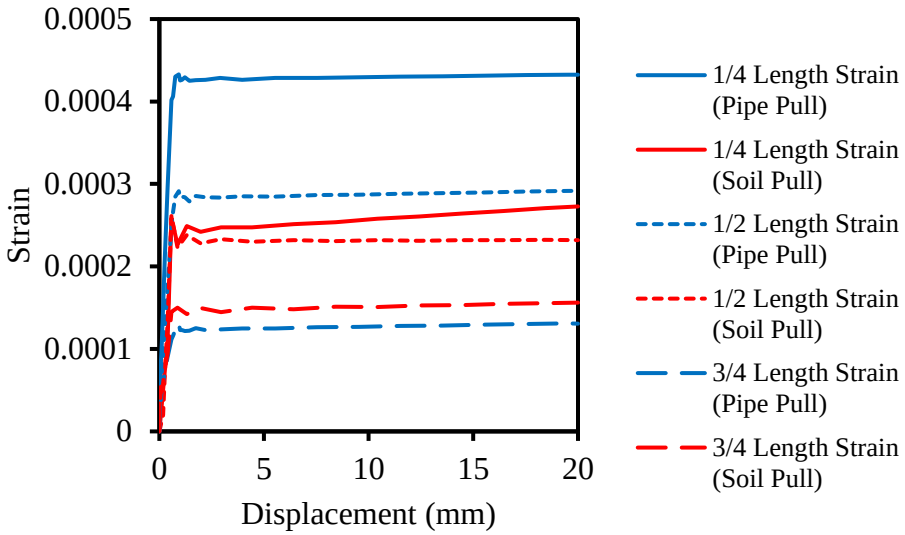

Fig. 4.19: Comparison of strain on 1m polyethylene pipe

The load-displacement responses for the longer pipes (i.e., 6.5 m) were nonlinear due to higher elongation for the pipe. The comparison of force-displacement responses of polyethylene pipe of 6.5 m length for soil pulling and pipe pulling simulation is shown in Figure 4.20. The maximum pull-out force for pipe pulling simulation occurs at a displacement of 9.3 mm, while the maximum pull-out force for soil pulling occurs at a displacement of 10.9 mm. The pipe pulling and soil pulling results are comparable at lower displacement (until a displacement of 1.3 mm), after which the pipe pulling predicts a higher pull-out force than soil pulling, resulting from the differences in the load transfer mechanisms.

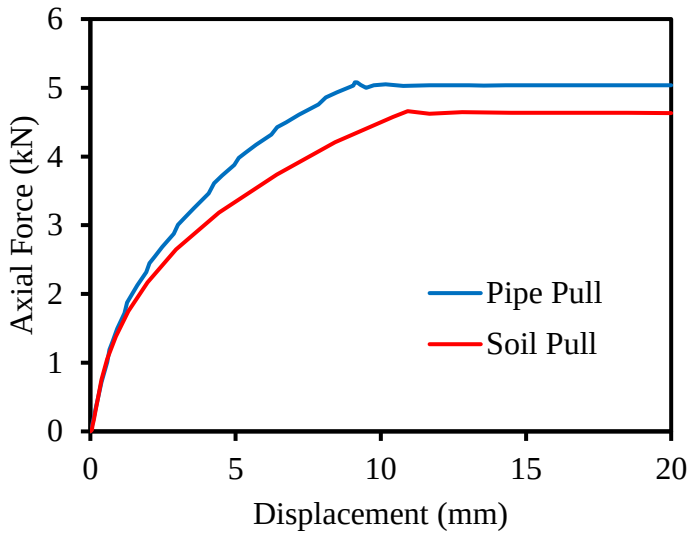

Fig. 4.20: Comparison of force-displacement relationship for a 6.5m polyethylene pipe

The load transfer mechanism for 6.5 m long pipe was also examined through an investigation of the strains along the length of the pipe. Figure 4.21 shows the comparison of strain developed on the modeled pipe during the FEA simulation. Tensile strains are observed on the pipe during the simulations. Note that strains at all three locations start immediately after application of soil movement during soil pulling. However, during pipe pulling, strains at the downstream points start at certain leading end displacements. At L/4, the highest tensile strain is observed, the amount of tensile strain on the pipe is reduced at L/2, and strain does not begin to develop until a displacement of 2 mm. At 3L/4, the tensile strain on the pipe further reduces, and strain does not begin to develop until a displacement of 4.4 mm. The behavior clearly demonstrates the differences in the load transfer mechanism for tests performed using different loading techniques (soil pull versus pipe pull).

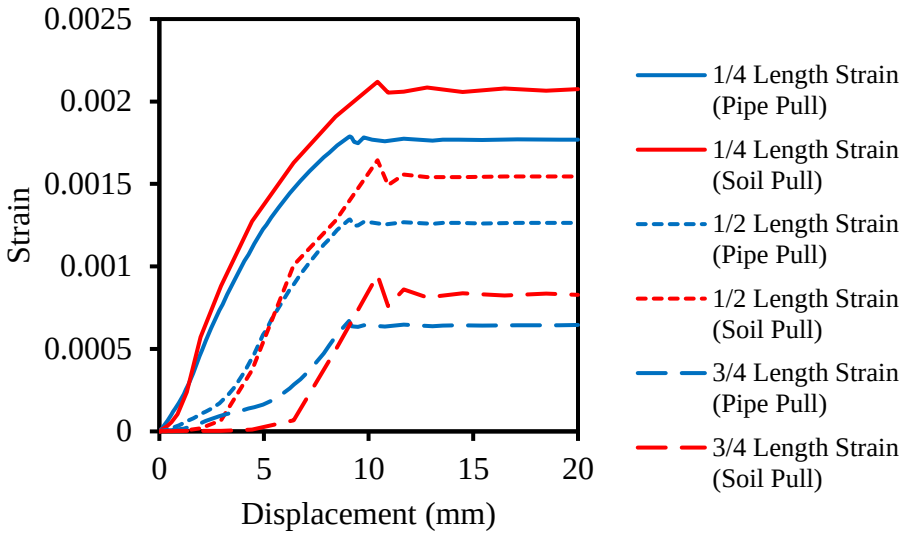

Fig. 4.21: Comparison of strain for 6.5m polyethylene pipe

4.3.2 Effect of soil width

The 1 m and 6.5 m pipe lengths were investigated for varying soil widths of 2 m, 4 m, 6 m to investigate the effect of test cell width in an experimental facility. Figure 4.22 shows the effect of soil width on a 1 m polyethylene pipe subjected to either soil pull or pipe pull. It shows that both soil pulling simulation and pipe pulling simulation calculate almost the same pull-out forces. The peak pulling forces do not change with the changes of soil width. Hence, increasing width beyond 2 m is of no significance for short polyethylene pipes.

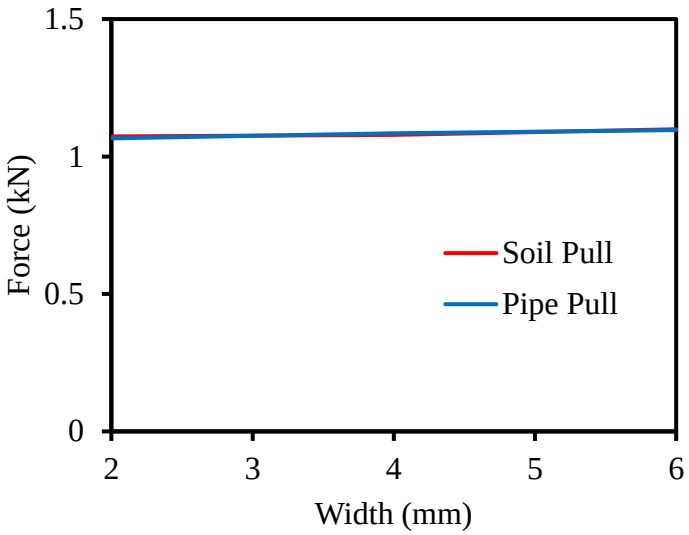

Fig. 4.22: Effect of soil width on 1m polyethylene pipe

Similar results were found for longer polyethylene pipes as shown in Figure 4.23. In Figure 4.23 the peak pull-out forces remain constant with increasing width. Thus, increasing width is not significant in the development of axial pull-out forces.

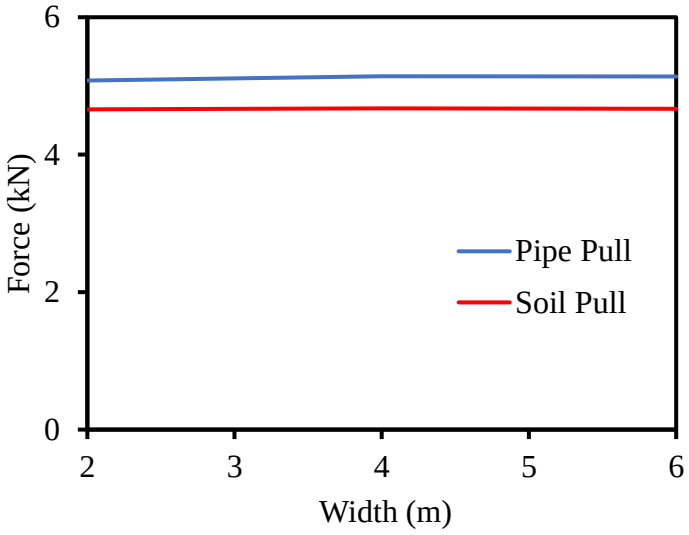

Fig. 4.23: Effect of soil width on 6.5 m polyethylene pipe

4.3.3 Effect of pipe diameter on axial pull-out force

The study evaluated the contribution of pipeline diameter on axial pull-out by simulating polyethylene pipes of 60 mm (small diameter) and 100 mm (large diameter) buried at 400 mm depth. Figure 4.24 shows the effect of diameter on axial pull-out force for 1 m long of pipe sample. The results show that the pull-out forces increase with an increase in diameter both for pipe pulling and soil pulling. This is because an increase in diameter provides an increased surface area for the soil-pipe interface, increasing the amount of interface shear strength mobilized due to the simulated ground movement. The peak pull-out forces for both soil pulling and pipe pulling for 1 m long pipes are almost the same irrespective of increases in pipe diameter, indicating no effect of pipe diameter on the results from soil pulling and pipe pulling.

The effect of pipe diameter on the pull-out forces obtained from the methods was also minimum for 6.5 m long pipe sample, as shown in Figure 4.25. Figure 4.25 shows that the peak pull-out force for the 60 mm pipe with pipe pulling is 8% higher than the peak pull-out force for soil pulling. The difference in result slightly reduces to 6% for the 100 mm diameter pipe.

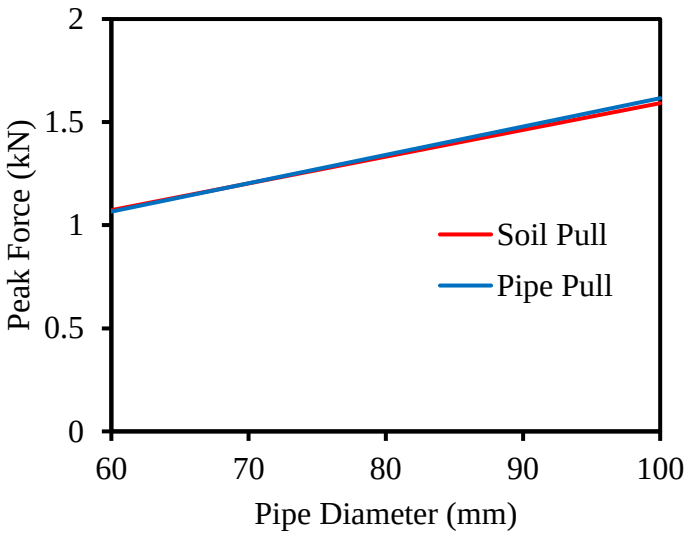

Fig. 4.24: Effect of diameter on the development of axial pullout force for 1m polyethylene pipe

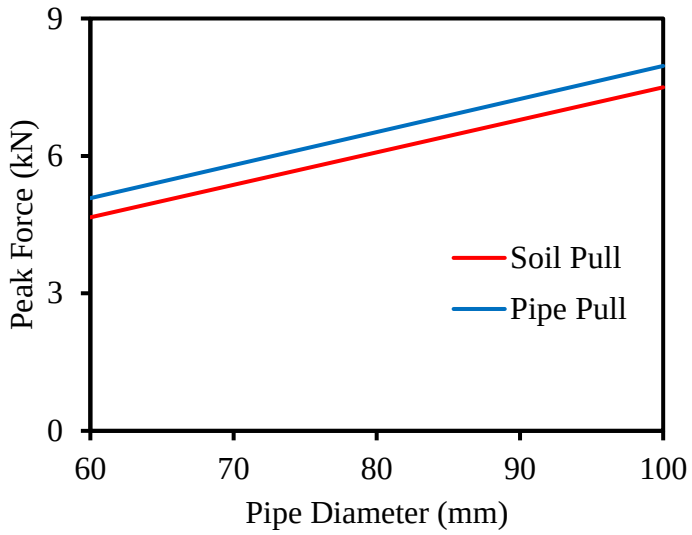

Fig. 4.25: Effect of diameter on the development of axial pullout force for 6.5m polyethylene pipe

4.3.4 Effect of burial depth

In this study, a comparison was made for effect of burial depth due to the simulation of soil pull and pipe pull. The simulation was achieved by simulating pipes of different lengths (1 m and 6.5 m) and different diameters (60 mm and 100 mm) buried at 400 mm and 600 mm, respectively. Figure 4.26 shows the comparison of results depicting the effect of burial depth for a 1 m long pipe. From the results, there is an increase in peak force with increasing burial depth; this is because of an increase in overburden pressure with an increase in depth. The results also show that pull-out forces from soil pulling and pipe pulling are comparable for both 60 mm and 100 mm diameter pipes, indicating no effect of burial depth on pull-out forces obtained from different

simulation methods. However, as discussed earlier, the pipe wall strain development may be different during pipe pulling and soil pulling. Pipe wall strains examined at different points along the length of pipes are provided in the Appendix, confirming the differences in the load transfer mechanism.

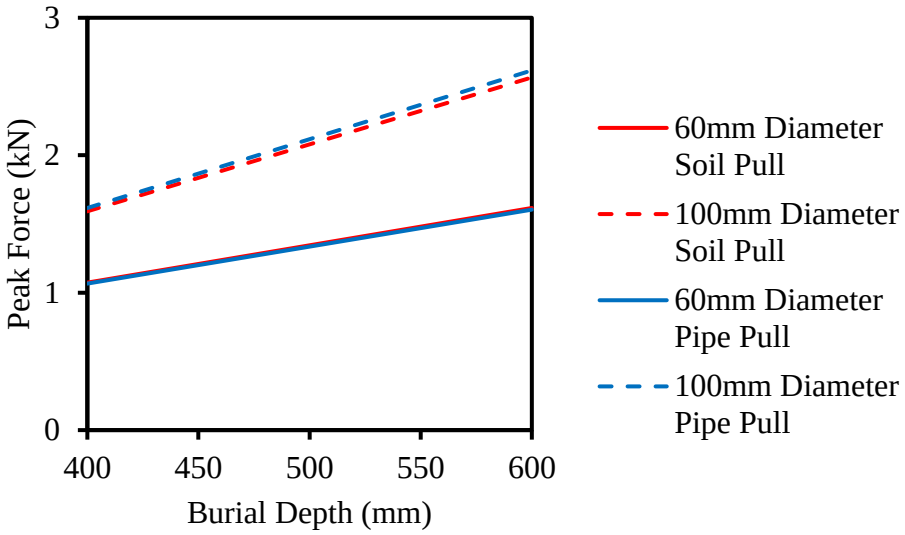

Fig. 4.26: Effect of burial depth on the development of axial pullout force for 1m polyethylene pipe

Figure 4.27 shows the comparison of results for the effect of burial depth on a 6.5 m long pipe. The peak force increases with an increasing burial depth confirming the observation in 1 m long pipes. However, the pipe pulling results are slightly higher than the soil pulling results for 60 mm and 100 mm diameter pipes.

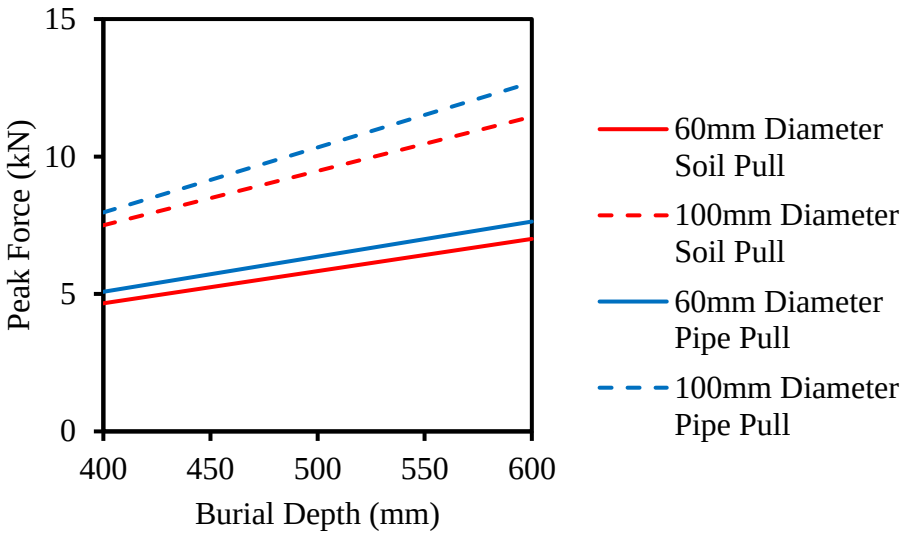

Fig. 4.27: Effect of burial depth on the development of axial pull-out force for 6.5m polyethylene pipe

4.3.5 Effect of internal pressure

This study investigated the effect of internal pressure on polyethylene pipes subjected to axial ground movement. A pressure of 700 kPa simulated water transportation through the 60 mm diameter polyethylene pipe buried at a depth of 400 mm, while a pressure of 2 MPa simulated gas transportation through the 60 mm diameter polyethylene pipe buried at a depth of 400 mm. Figures 4.28 and 4.29 show the force-displacement diagram for a 1 m and 6.5 m long steel pipe, respectively. The figure compares soil pulling and pipe pulling for no internal pressure case and internal pressure cases.

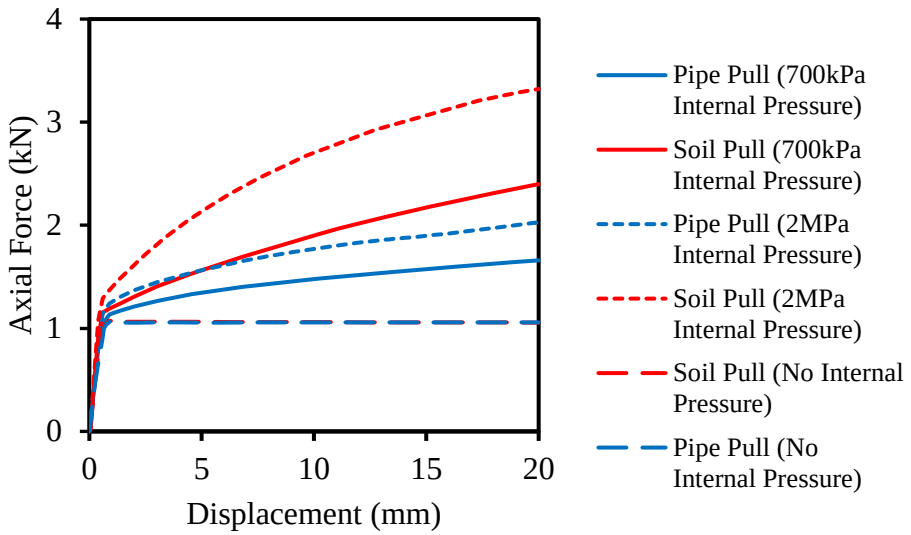

Fig. 4.28: Effect of internal pressure on the development of axial pullout force for 1m polyethylene pipe

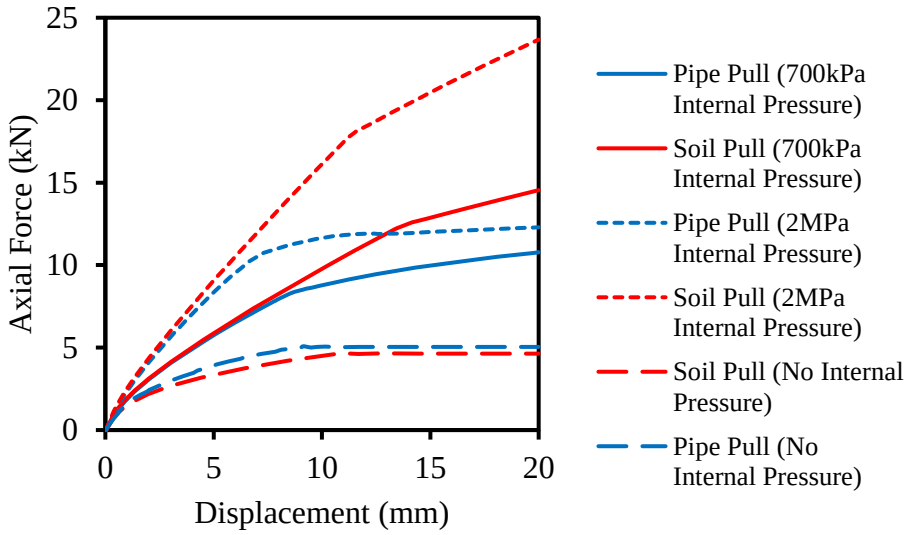

Fig. 4.29: Effect of internal pressure on the development of axial pullout force for 6.5m polyethylene pipe

Figures 4.28 and 4.29 reveal that the pull-out force can be significantly higher for the pipe with an internal pressure than the pipe without internal pressure for polyethylene pipes. Due to the internal

pressure, the pipe diameter can be increased that may increase contact pressure and hence the pull-out resistance. In Figure 4.28 the development of axial pull-out for a 1m polyethylene pipe is comparable till a displacement of 0.9 mm is achieved after which the peak force continues to increase with an increase in internal pressure. The peak force continues to develop until the displacement reaches 20 mm, and the force due to soil pulling is higher than the force due to pipe pulling for both internal pressures.

The development of axial pull-out for a 6.5 m polyethylene pipe is comparable till a displacement of 1.2 mm is achieved, after which the peak force continues to increase with an increase in internal pressure, as earlier discussed for the 1 m pipe, the peak force is not achieved until the displacement reaches 20 mm (Figure 4.29). The soil pulling results are higher than the pipe pulling results for both internal pressures.

CHAPTER FIVE

CONCLUSIONS AND RECOMMENDATION

5.1 Overview

Pipelines are sometimes unavoidably routed through areas susceptible to geohazards. During geohazard events, loads are developed on the buried pipes, threatening the pipeline's service requirements. Pipelines are designed based on the maximum load expected during the service life of the pipeline. Hence it is essential to determine the accurate maximum load to ensure a safe design. Many experimental studies have attempted to determine the maximum load on pipelines subjected to axial ground movement. However, the method adopted in the laboratory (pulling pipe through soil) is different from the actual way ground movement occurs in the field where unstable soil mass moves away from stable soil mass. Therefore, the principal objective of this study was to compare laboratory techniques to actual real-life ground movement scenarios using finite element analysis. In this chapter, conclusions from this study are presented.

5.2 Conclusions

The key findings from this study are discussed below:

- An increase in pipeline length increases the peak load on the pipeline due to an increase in frictional length of the soil-pipeline interface.
- An increase in width beyond 2 m does not significantly affect the peak axial force on a pipeline.
- An increase in pipeline diameter increases the peak load on the pipeline, which is due to an increase in surface area of the soil-pipe interface.

- An increase in pipeline burial depth increases the peak load on the pipeline, which is due to an increase in soil overburden pressure.
- In short steel pipelines, the elongation of pipe and pipe diameter reduction is more due to soil pulling than pipe pulling. This effect makes the load developed in short steel pipes lower for soil pulling compared to pipe pulling loads.
- In long steel pipelines, pipe elongation and pipe diameter reduction are more due to pipe pulling than soil pulling. This effect makes the load developed in long steel pipes higher for soil pulling compared to pipe pulling.
- There is no significant change in peak load in steel pipelines due to internal pressure in short and long pipes.
- In short polyethylene pipelines, the elongation of pipe and pipe diameter reduction is more due to pipe pulling than soil pulling. This effect makes the load developed in short polyethylene pipes comparable for both pipe pulling and soil pulling.
- In long polyethylene pipelines, the elongation of pipe and pipe diameter reduction is more due to soil pulling than pipe pulling. This effect makes the load developed in long polyethylene pipes lower for soil pulling than pipe pulling.
- The peak load developed in polyethylene pipes, due to internal pressure, increases with increasing internal pressure. Also, for polyethylene pipelines the pipe pulling loads are lower than soil pulling loads.
- Overall, although the pull-out might be the same from pipe pull and soil pull, depending upon other parameters (pipeline length, diameter, and material), the load transfer mechanisms are different for the two approaches of loading.

The major contribution of this thesis is the significance of length of pipe in forces developed due soil-pipe interaction. With varying length, the laboratory idealization and field idealization predict different results. Therefore, the following recommendations are made:

5.3 Recommendations

The following study could be adopted as a follow up to this study:

- Full-scale experiments can be conducted by pulling the soil mass instead of the current experimental technique adopted in the laboratory.
- The current study used finite element analysis to investigate the effect of length, pipe diameter, burial depth, and internal pressure on the development of axial pull-out. The effects of frictional factors and operational temperature were not investigated. These effects could be investigated in more detail in future research. Longer lengths from 10 m can also be investigated.
- Numerical studies could be conducted to compare the development of pull-out of buried pipes subjected to lateral, and upheaval ground movement.
- The cyclic loading of the pipeline could be modeled by intermittently changing the direction of pulling to simulate the cyclic load.
- In this study, the behaviour of soil was modeled using the Mohr-Coulomb model. A more advanced model could be used to model the constitutive behaviour of the soil.

References

Abaqus, 2016. Abaqus user's guide. Dassault Systems. Available on http://130.149.89.49:2080/v2016/books/usb/default.htm

American Lifelines Alliance. 2001. Guidelines for the design of buried steel pipe. American Lifelines Alliance in partnership with the Federal Emergency Management Agency and American Society of Civil Engineers, Washington, D.C. Available on www.americanlifelinesalliance.org [accessed 14th March 2021]

Almahakeri, M., Moore, I. D., Fam, A., 2016. Numerical study of longitudinal bending in buried GFRP pipes subjected to lateral earth movements. Journal of Pipeline Systems Engineering and Practice, **8**(1): 04016012-1-12. doi: 10.1061/(ASCE)PS.1949-1204.0000237.

ASCE. (1984). Guidelines for the seismic design of oil and gas pipeline systems. Prepared by the Committee on Gas and Liquid Fuel Lifelines pf the ASCE Technical Council on Lifeline Earthquake Engineering, New York.

Audibert, J.M.E. and Nyman, K.J. (1977). Soil restraint against horizontal motion of pipes. Journal of the Geotechnical Engineering Division, ASCE, Vol. 103, No.GT10, pp. 1119-1142.

Bilgin, O. and Stewart, H. E., 2009. Pullout resistance characteristics of cast iron pipe. Journal of Transportation Engineering, **135**(10): 730-735.

Bolton, M. D., 1986. The strength and dilatancy of sands. Geotechnique, **36**(1): 65-78. doi: 10.1680/geot.1986.36.1.65.

Bughi, S., Aleotti, P., Bruschi, R., Andrei, G., Milani, G. and Scarpelli, G., 1996. Slow movements of slopes interfering with pipelines: modeling and monitoring. Proceedings of the 15th International Conference on Offshore Mechanics and Arctic Engineering, June 16 -20, Vol. 5, ASME, Florence, Italy, pp. 363-372.

Cappelletto, A., Tagliaferri, R., Guirlani, G., Andrei, G., Furlani, G. and Scarpelli, G., 1998. Field full scale tests on longitudinal pipeline-soil interaction. Proceedings of International Pipeline Conference, Calgary, Alberta, ASME, Vol. 2, pp.771-778.

Daiyan, N., Kenny, S., Phillips, R., and Popescu, R., 2010. Numerical investigation of oblique pipeline/soil interaction in sand. Proceedings of the 8th International Pipeline Conference, Calgary, Alberta, ASME, IPC2010-31644

Das, B. M., 2008. Advanced soil mechanics, 4th Edition. CRC Press, Taylor & Francis Group. ISBN 13:978 1-4822-3483-1, pp 405-413

Guo, P. J. and Stolle, D. F. E. 2005. Lateral pipe-soil interaction in sand with reference to scale effect. Journal of Geotechnical and Geoenvironmental Engineering. ASCE, 131(3): 338-349

Hardin, B. O., and Black, W. L., 1966. Sand stiffness under various triaxial stress. Journal of the Soil Mechanics and Foundations Division. ASCE, 92(SM2): 27-42

Janbu. N. 1963. Soil compressibility as determined by oedometer and triaxial tests. In Proceedings, European Conference on Soil Mechanics and Foundations Engineering. Wiesbaden, Germany. Vol. 1, pp. 19-25

Jung, J., O'Rourke, T., and Olson, N. 2013. Lateral soil-pipe interaction in dry and partially saturated sand. Journal of Geotechnical and Geoenvironmental Engineering. 139(12): 2028-2036

Karimian, H. 2006. Respoonse of buried steel pipelines subjected to longitudinal and transverse ground movement, Ph.D. thesis. Department of Civil Engineering, The University of British Columbia, Vancouver, B.C.

Kroon, D. H., Linemuth, D. D., Sampson, S. L., Vincenzo, T., 2004. Corrosion protection of ductile iron pipe. Corrosion (2004)- Conference: 1-17. doi: 10.1061/40745(146)75.

McAllister, E. W. (2001). Pipeline rules of thumb handbook, Gulf Professional Publishing, 648 p.

Meidani, M., Meguid, A. M., Chouinard, E. L., 2017. Evaluation of soil-pipe interaction under relative axial ground movement. Journal of Pipeline Systems Engineering and Practice. 8(4): 04017009-1-10. doi: 10.1061/(ASCE)PS.1949-1204.0000269

Mitchell, J. K., 1963. Current lunar soil research. Journal of the Soil Mechanics and Foundations Division. Vol. 90, Issue 3. https://doi.org/10.1061/JSFEAQ.0000626

Muntakim, A. H., Dhar, A. S., 2018. Investigation of axial pullout behavior of buried polyethylene pipelines. Newsletter, International Association for Computer Methods and Advances in Geomechanics, Vol.23.

Murugathasan, P., Dhar, A. S., Hawlader, B. C., 2019. An experimental and numerical investigation of pullout behavior of ductile iron water pipes buried in sand. Canadian Journal of Civil Engineering. 48(2): 134-143. https://doi.org/10.1139/cjce-2019-0366

Paulin, M. J., Phillips, R., Clark, J. I., Trigg, A., Konuk, I., (1998). A full-scale investigation into pipeline/soil interaction. Proceedings of International Pipeline Conference, ASME, Calgary, AB., pp. 779-788.

Pipeline Research Council International (PRCI), 2009. Guidelines for constructing natural gas and liquid hydrocarbon pipelines through areas prone to landslide and subsidence hazards. Chantilly, VA: C-CORE, D. G. Honegger Consulting, and SSD.

PIPA (2001) Polyolefins technical information. Plastics Industry Pipe Association of Australia, Available from: www.pipe.com.au (Accessed August 2019)

Reza, A., Dhar, A. S., (2021). Axial pullout behavior of buried medium-polyethylene gas distribution pipes. International Journal of Geomechanics. 21(7): 04021120-1-13. doi: 10.1061/(ASCE)GM. 1943.5622.0002101

Rizkalla, M., Trigg, A., Simmonds, G., 1996. Recent advances in the modeling of longitudinal pipeline-soil interaction for cohesive soils. Rep. No. CONF-9606279. New York, ASME.

Rowe. P. W., 1962. The stress-dilatancy relation for static equilibrium of an assembly of particles in contact. Proceedings of the Royal Society A: Mathematical, Physical and Engineering Sciences. Vol. 269, Issue 1339. https://doi.org/10.1098/rspa.1962.0193

Roy, K., Hawlader, B., Kenny, S., Moore, I., 2015. Finite element modeling of lateral pipeline-soil interactions in dense sand. Canadian Geotechnical Journal. 53(3): 490-504. doi.org/10.1139/cgj-2015-0171

Saha, R. C., Dhar, A., Hawlader, B. 2019. Shear strength assessment of a well-graded clean sand. Annual conference of Canadian Geotechnical Society, GeoStJohn's 2019, St John's, NL, Canada

Sheil, B. B., Martin, C. M., Bryne, B. W., Plant, M., Williams, K., and Coyne, D. 2018. Full-scale laboratory testing of a buried pipeline in sand subjected to cyclic axial displacements. Geotecnique, 68(8): 684-698. doi.org/10.1680/jgeot.16.P.275

Trautmann, C. H. and O'Rourke, T. D., 1983. Behavior of pipe in dry sand under lateral and uplift loading. Geotechnical Engineering Report 83-7, Cornell University, Ithaca. NY.

Trautmann, C. H. and O'Rourke, T. D., 1985. Lateral force-displacement response of buried pipe. Journal of Geotechnical Engineering, 111(9): 1077-1093.

Trautmann, C. H., O'Rourke, T. D., Kulhawy, F. H., 1985. Uplift force-displacement response of buried pipe. Journal of Geotechnical Engineering, 111(9): 1061-1076

Trigg, A., and Rizkalla, M., 1994. Development and application of a closed form technique for the preliminary assessment of pipeline integrity in unstable slopes. International Conference on Offshore Mechanics and Arctic Engineering (OMAE-13), Houston, TX.

Weerasekara, L. (2007). Response of buried natural gas pipelines subjected to ground movements, M.A.Sc thesis, Department of Civil Engineering, University of British Columbia, Vancouver, B.C., Canada, 243 p.

Wijewickreme, D., Honegger, D., Mitchell, A., Fitzell, T., 2005. Seismic vulnerability assessment and retrofit of a major natural gas pipeline system: A case history. Earthquake Engineering Research Institute, Oakland, CA. Vol. 21, pp 539-567

Wijewickreme, D., Karimian, H., Honegger, D., 2009. Response of buried steel pipelines subjected to relative axial soil movement. Canadian Geotechnical Journal. 46(7): 735-752. https:/doi.org/10.1139/T09-019

Yimsiri, S., Soga, K., Yoshizaki, K., Dasari, G., O'Rourke, T., 2004. Lateral and upward soil-pipeline interactions in sand for deep embedments conditions. Journal of Geotechnical and Geoenvironmental Engineering. 130(8): 830-842. doi: 10.1061/(ASCE)10900241(2004)130:8(830)

APPENDIX A: Strains on steel pipe

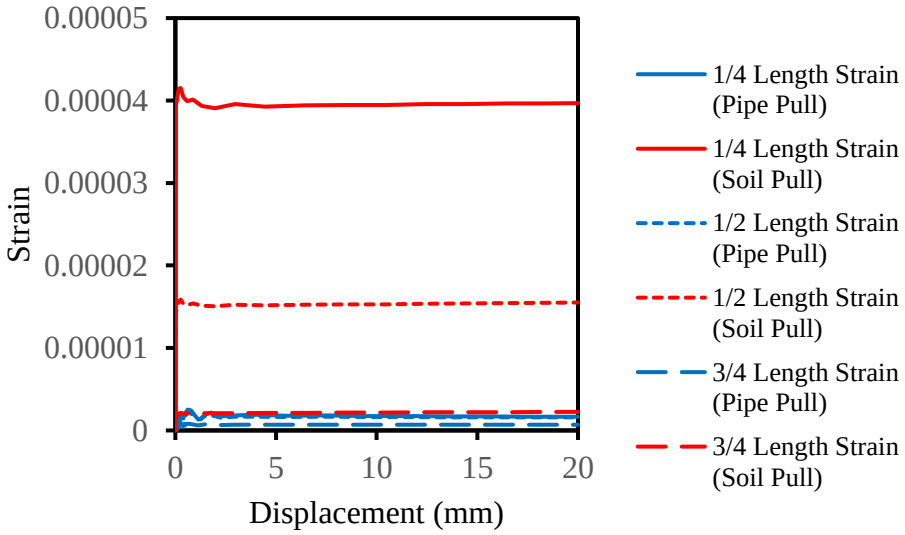

1 m length, 60 mm diameter steel pipe

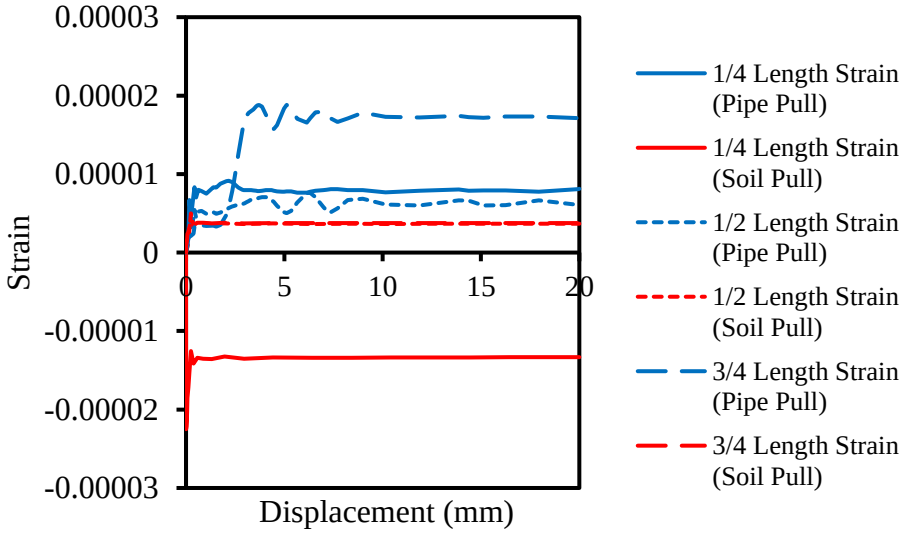

6.5 m length, 60 mm diameter steel pipe

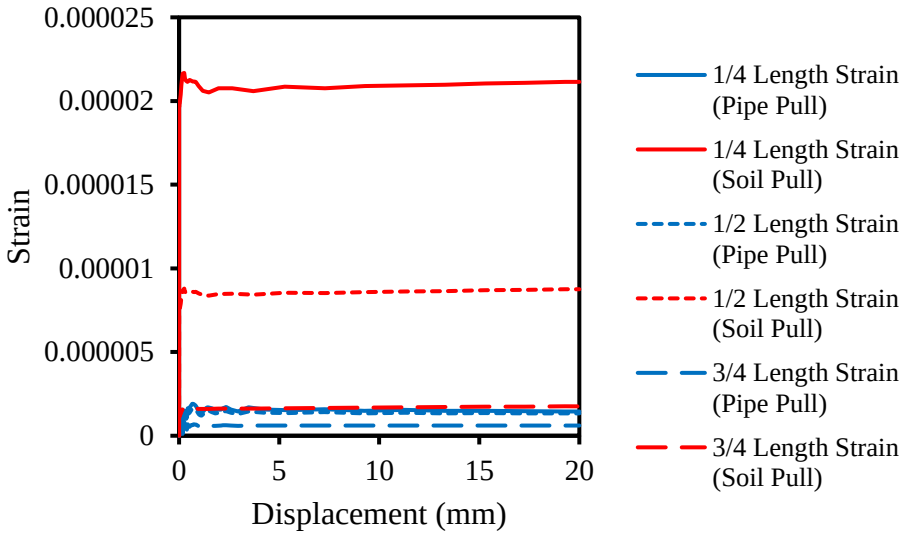

1 m length, 100 mm diameter steel pipe

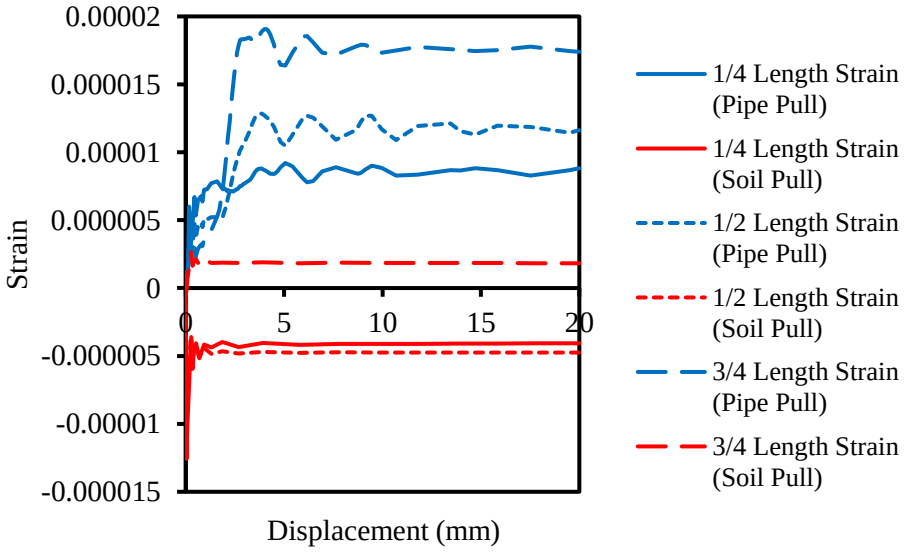

6.5 m length, 100mm diameter steel pipe

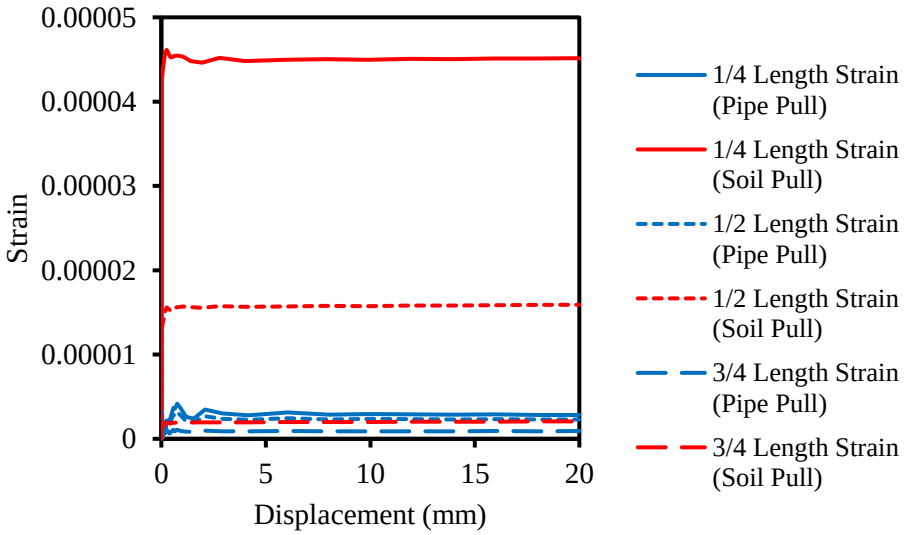

1m length, 60 mm steel pipe buried at a depth of 600 mm

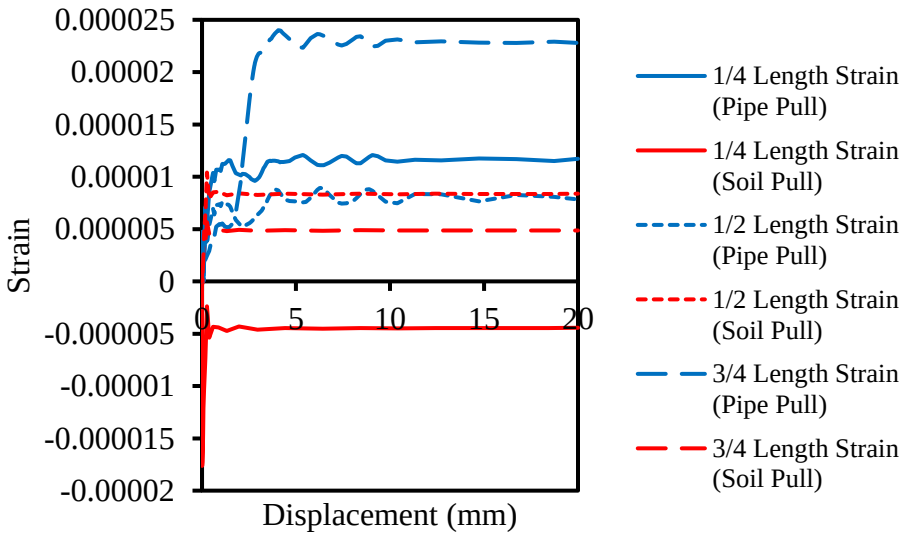

6.5 m length, 60 mm steel pipe buried at a depth of 600 mm

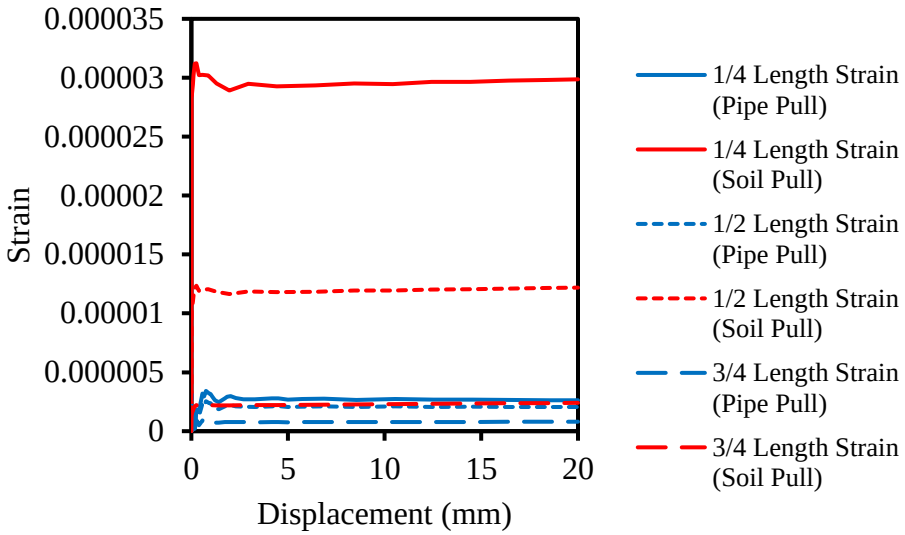

1 m length, 100 mm diameter steel pipe buried at a depth of 600 mm

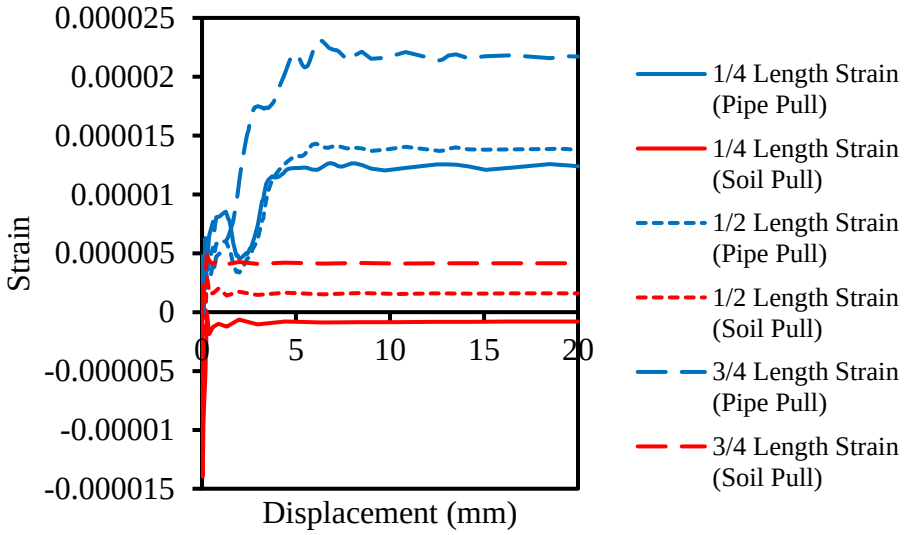

6.5 m length, 100 mm diameter steel pipe buried at a depth of 600mm

APPENDIX B: Stresses on polyethylene pipe

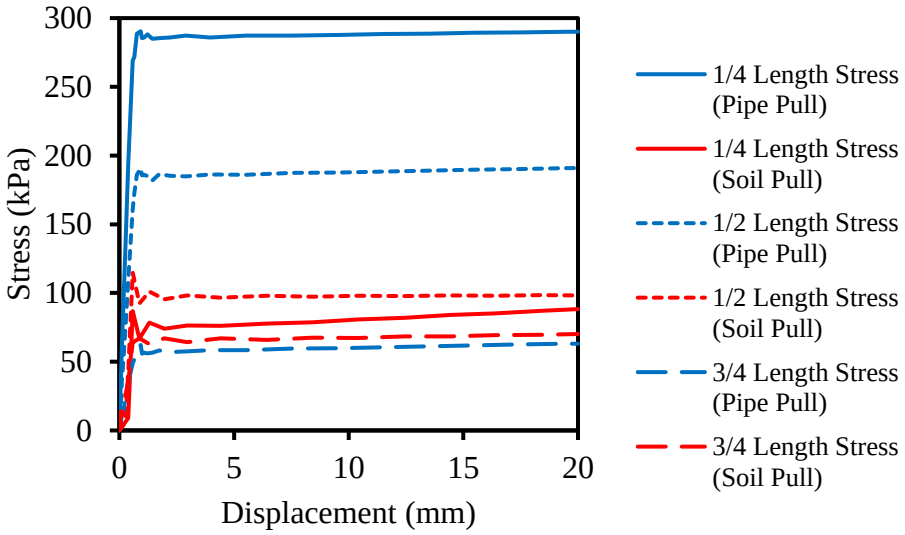

1 m length, 60 mm diameter polyethylene pipe

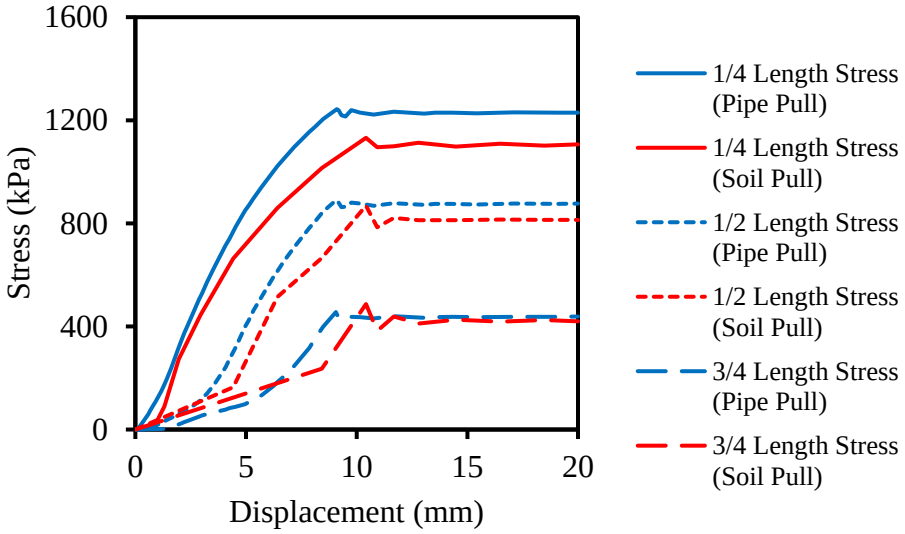

6.5 m length, 60 mm diameter polyethylene pipe

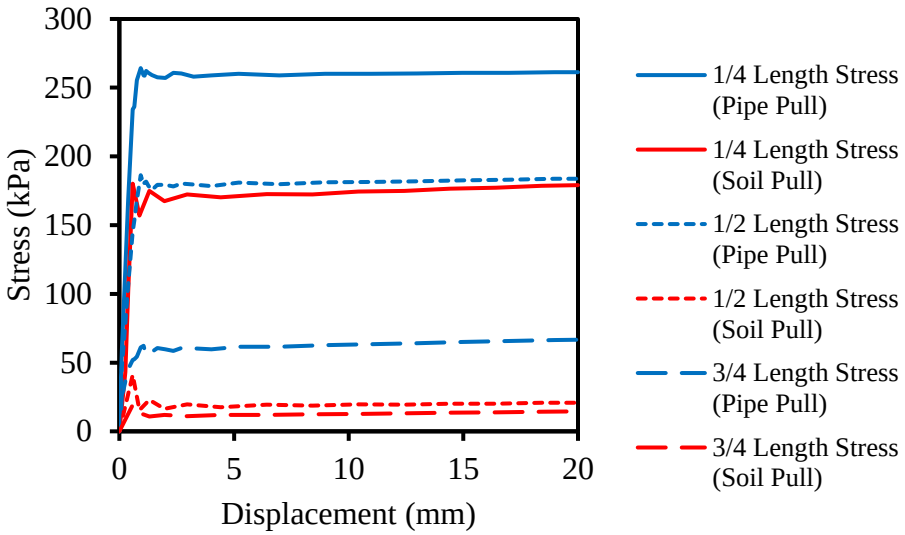

1 m length, 100 mm diameter polyethylene pipe

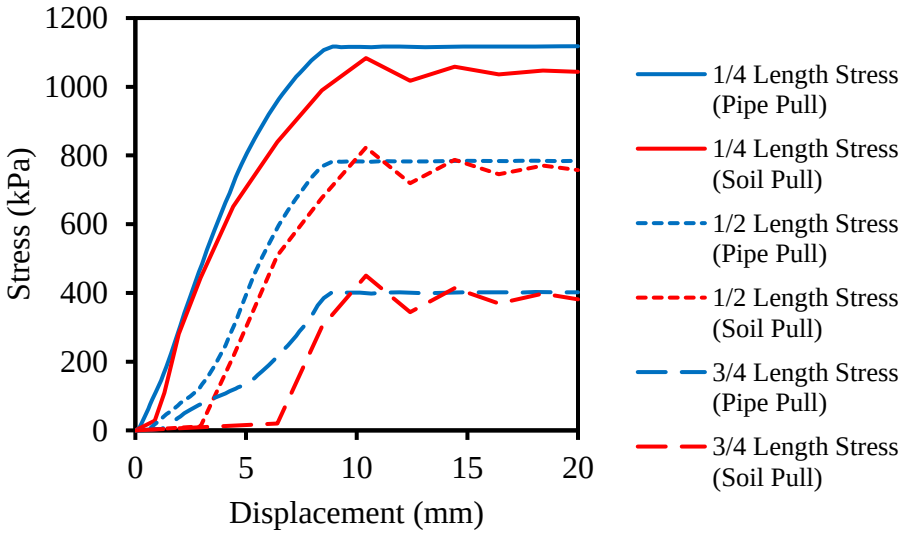

6.5 m length, 100 mm diameter polyethylene pipe

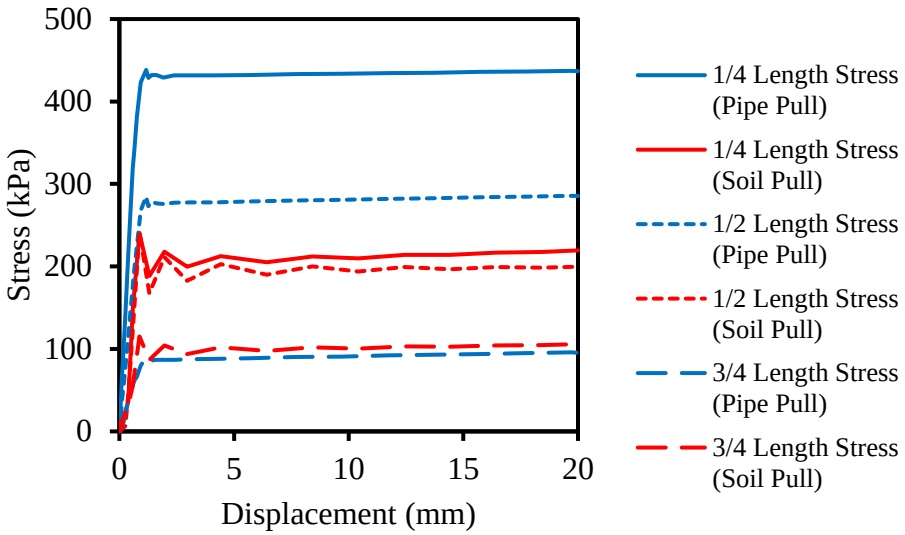

1 m length, 60 mm diameter polyethylene pipe buried at a depth of 600 mm

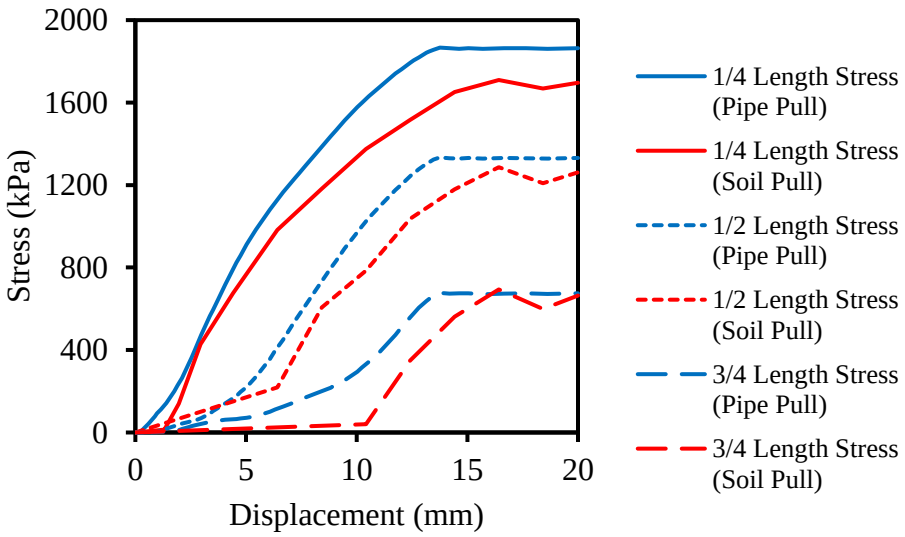

6.5 m length, 60 mm diameter polyethylene pipe buried at a depth of 600 mm

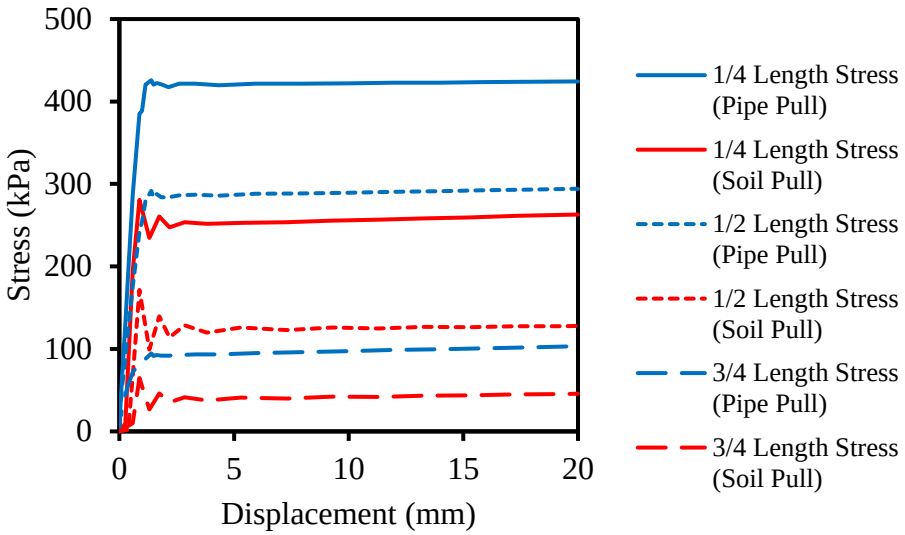

1 m length, 100 mm diameter polyethylene pipe buried at a depth of 600 mm

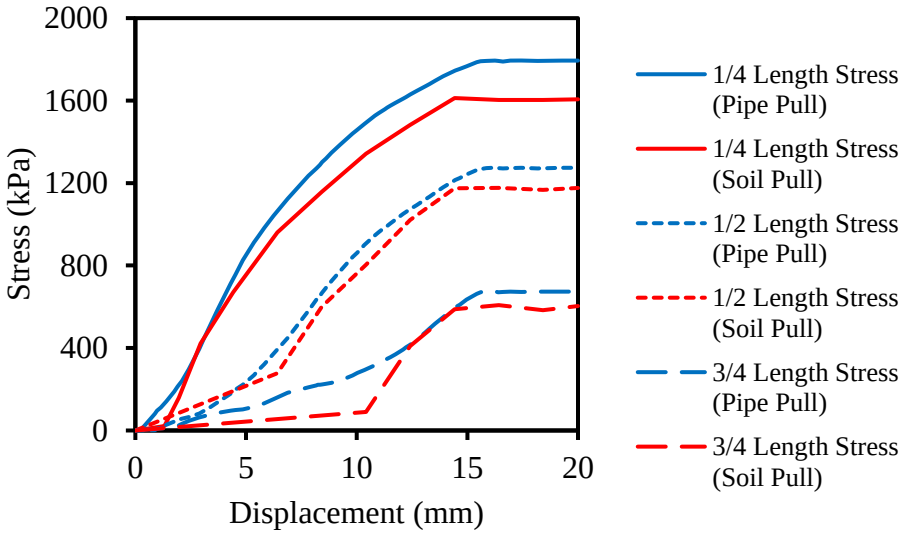

6.5 m length, 100 mm diameter polyethylene pipe buried at a depth of 600 mm

APPENDIX C: Stresses on Steel Pipe

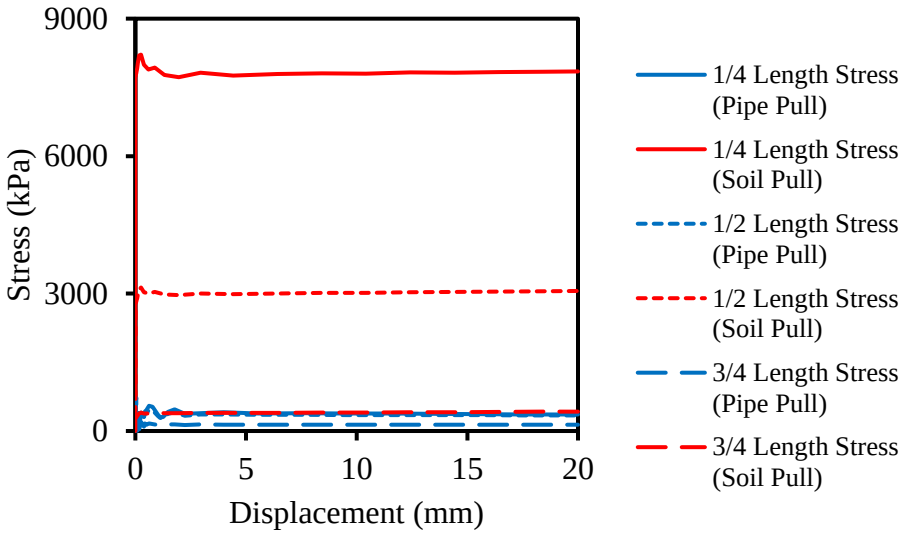

Comparison of stress on 1 m steel pipe

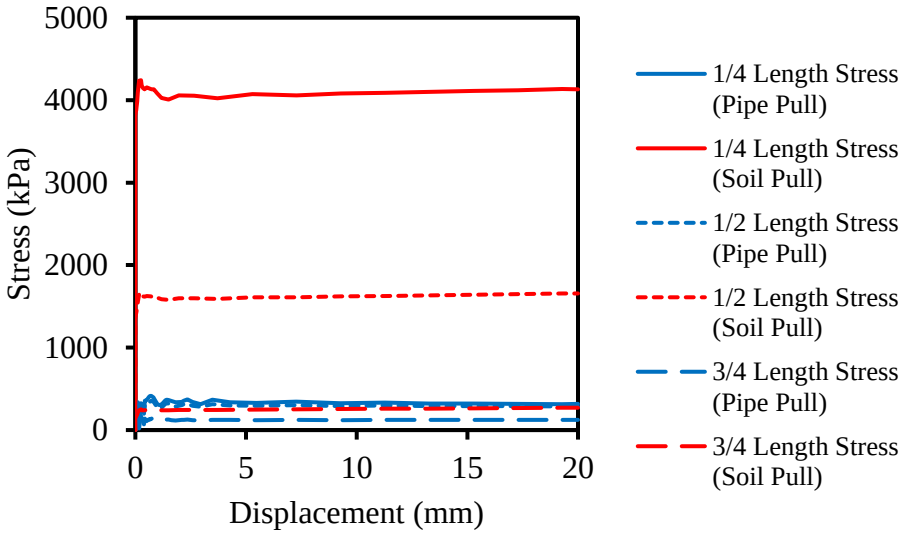

Comparison of stress on a 1 m long, 100 mm diameter steel pipe

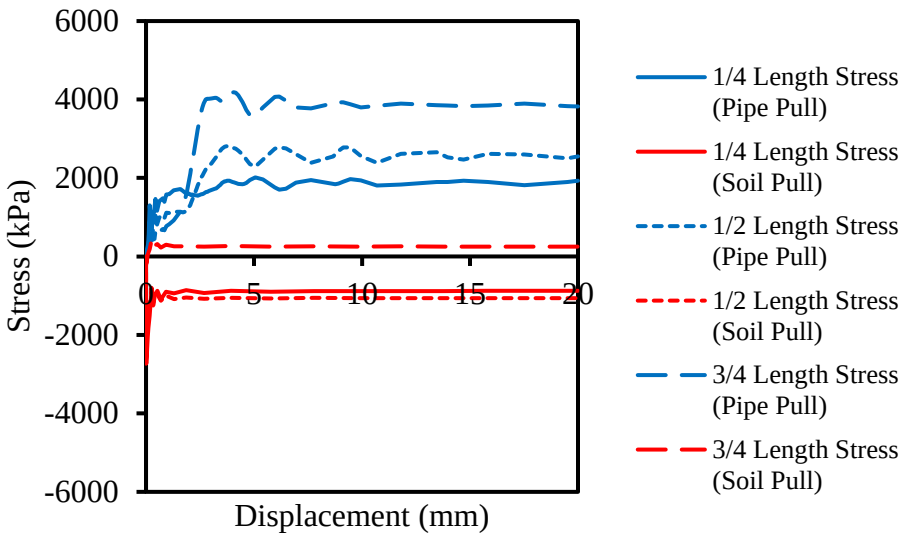

Comparison of stress on a 6.5 m long, 100 mm diameter steel pipe

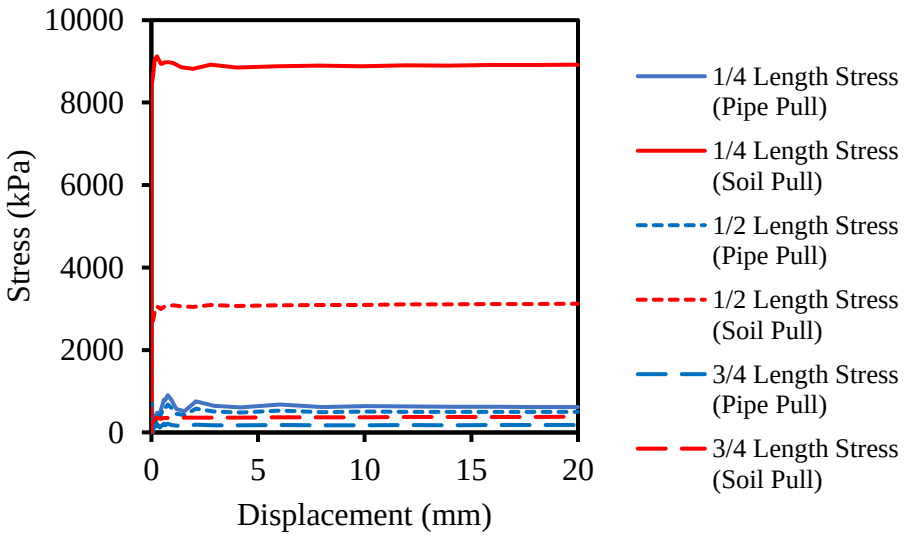

Comparison of stress on 1m long, 60mm diameter steel pipe buried at a depth of 600mm

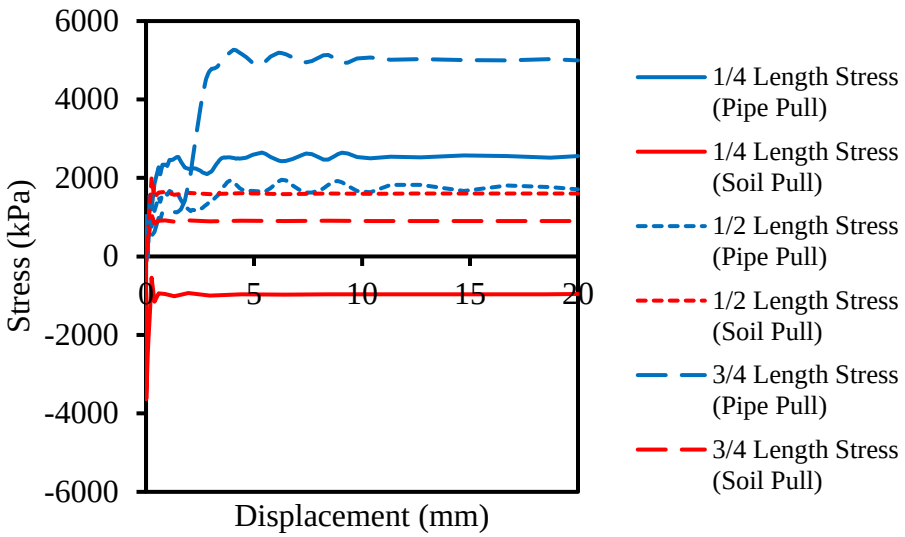

Comparison of stress on a 6.5m long, 60mm diameter steel pipe buried at a depth of 600mm

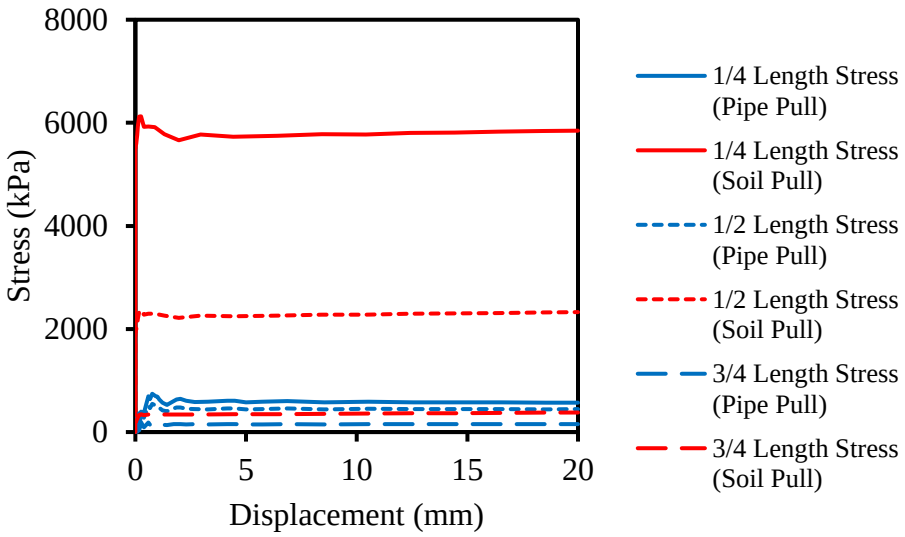

Comparison of stress on a 1m long, 100mm diameter steel pipe buried at a depth of 600mm

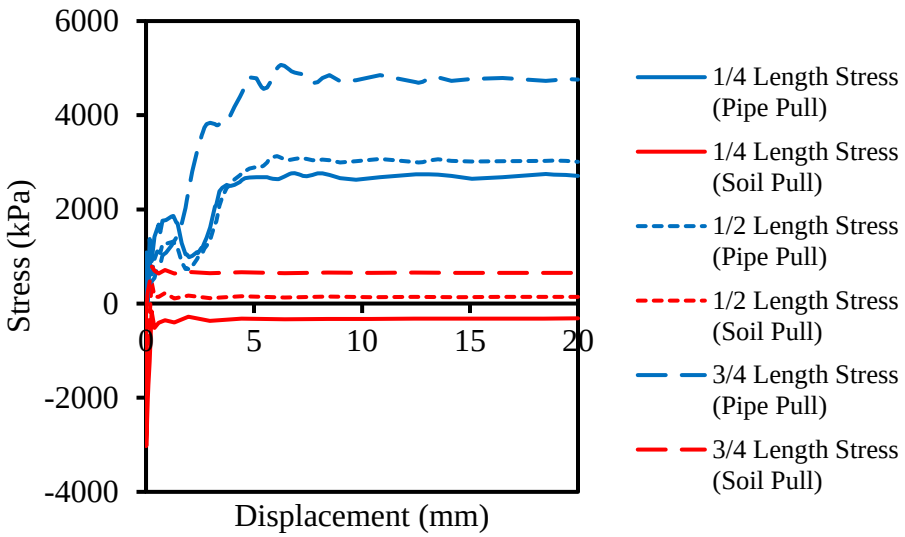

Comparison of stress on 6.5m long, 100mm diameter steel pipe buried at a depth of 600mm

APPENDIX D : Strains on Polyethylene pipes

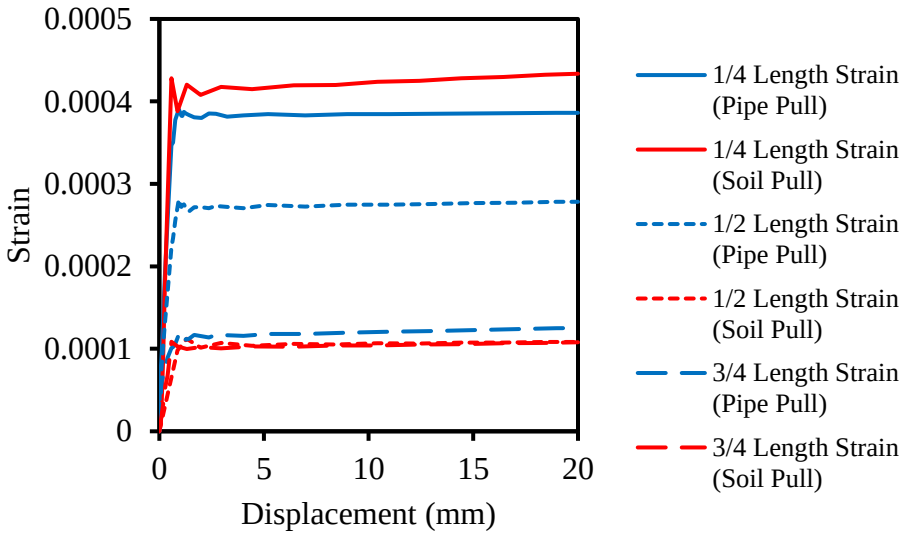

Comparison of strain for 1m long, 100mm diameter polyethylene pipe

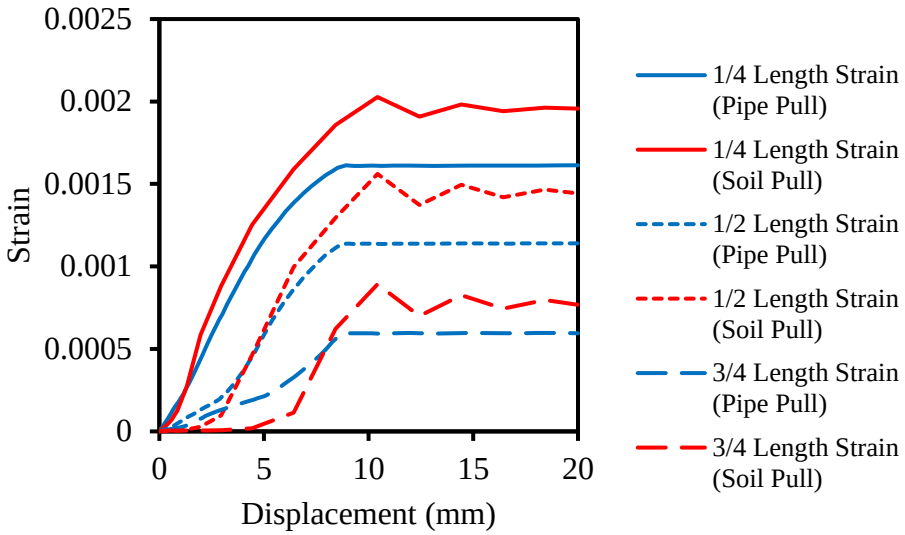

Comparison of strain on 6.5m long, 100mm diameter polyethylene pipe

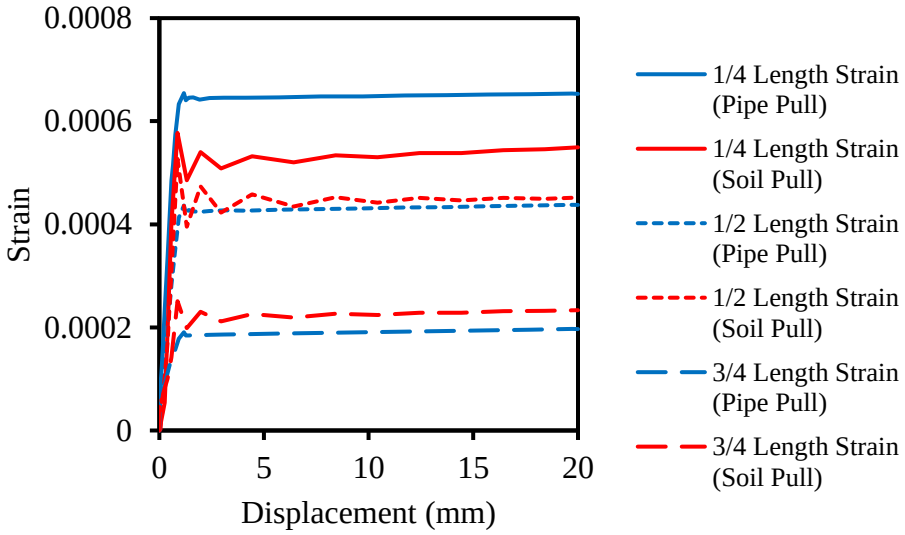

Comparison of strain on 1m long, 60mm diameter polyethylene pipe buried at a depth of 600mm

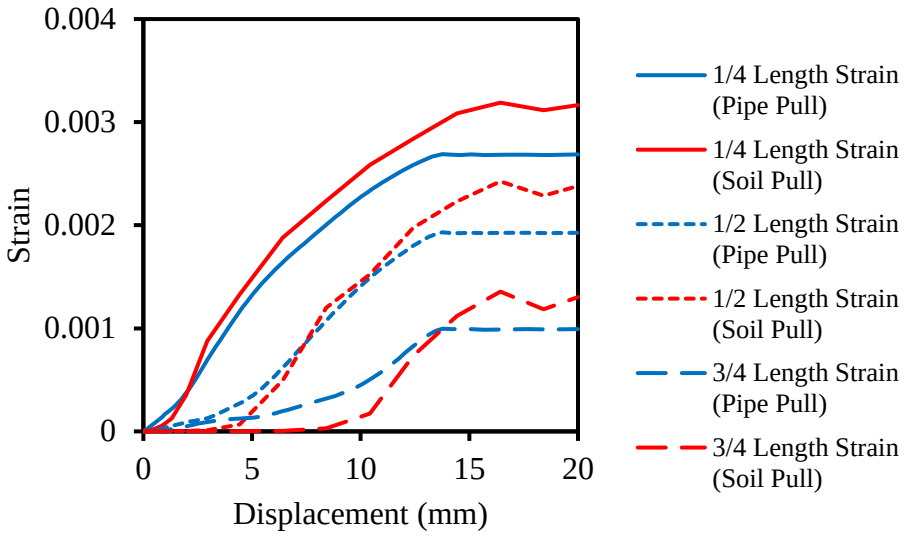

Comparison of strain on 6.5m long, 60mm diameter polyethylene pipe buried at a depth of 600mm

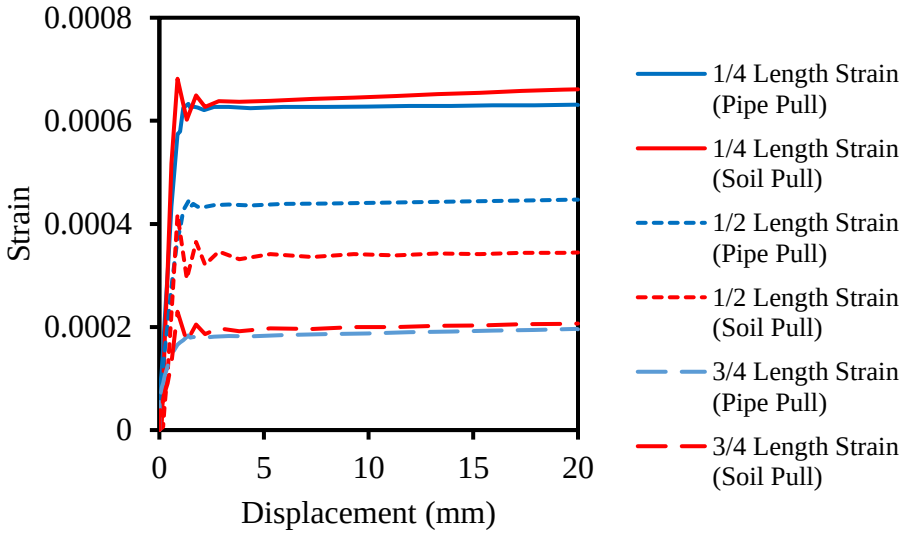

Comparison of strain on 1m long, 100mm diameter polyethylene pipe buried at a depth of 600mm

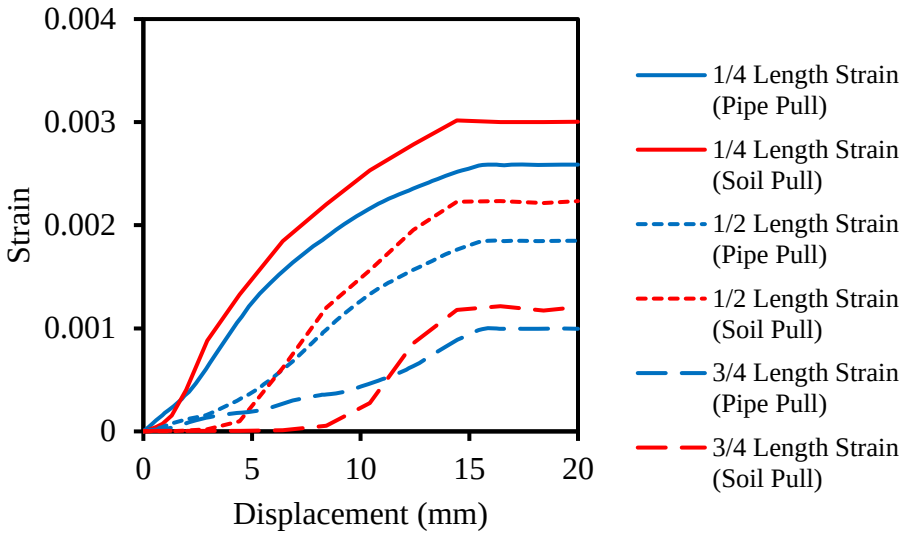

Comparison of strain on 6.5m long, 100mm diameter polyethylene pipe buried at a depth of 600mm

APPENDIX E : Force-Displacement Response of Pipes

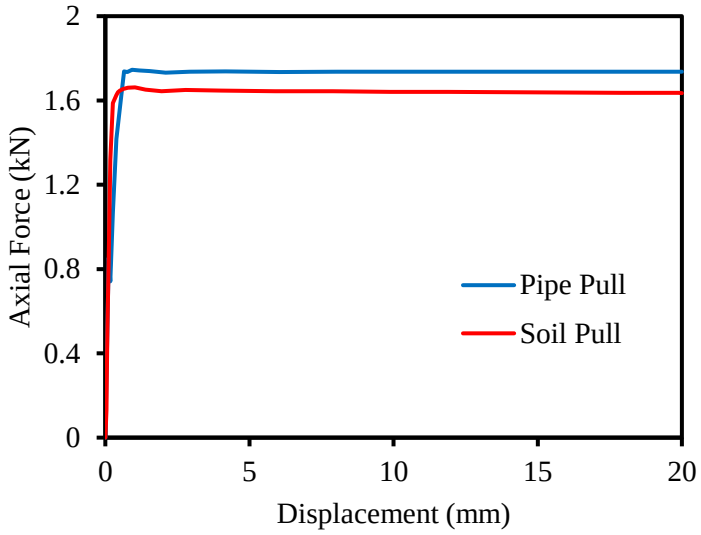

Comparison of Force-Displacement relationship of a 1m long, 60mm diameter steel pipe buried at a depth of 600mm

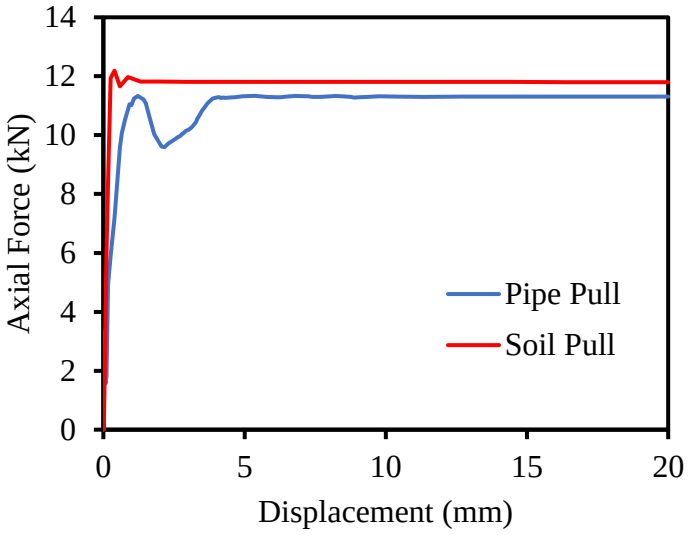

Comparison of Force-Displacement relationship for a 6.5m long, 60mm diameter steel pipe buried at a depth of 600mm

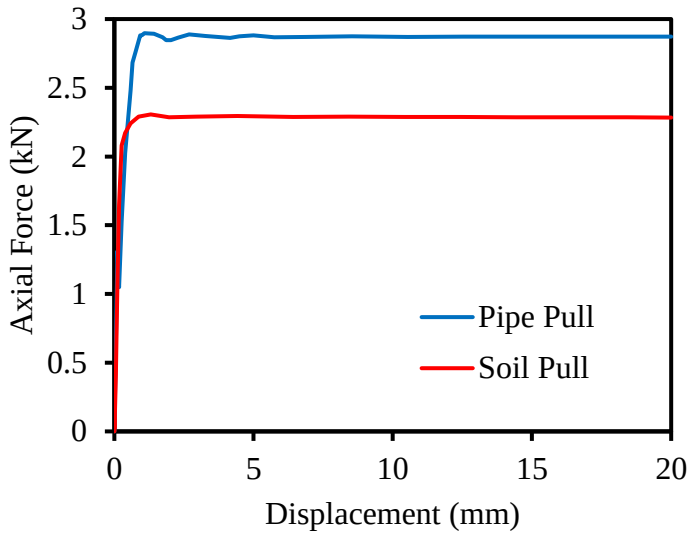

Comparison of Force-Displacement relationship for 1m long, 100mm diameter steel pipe buried at a depth of 600mm

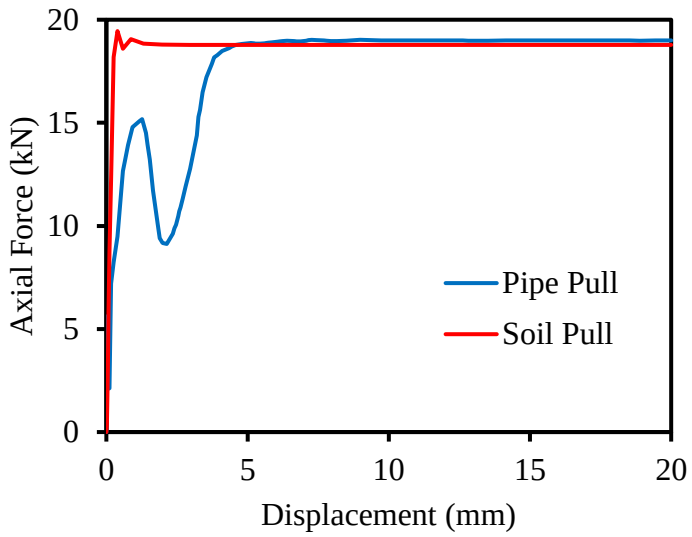

Comparison of Force-Displacement relationship for 6.5m long, 100mm diameter steel pipe buried at a depth of 600mm

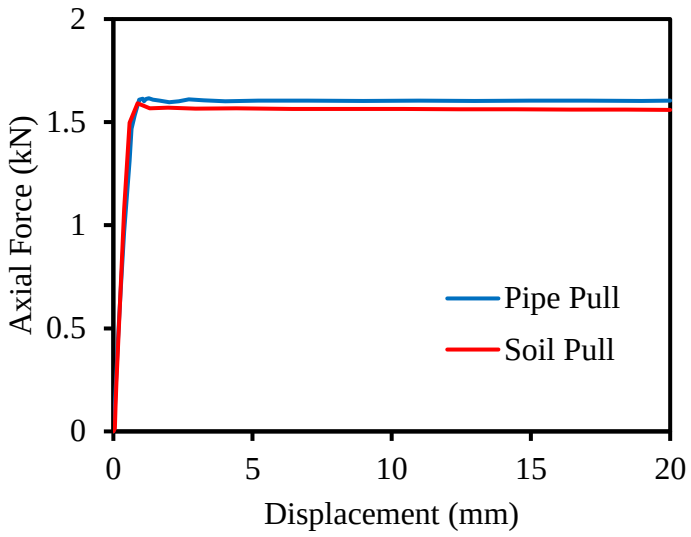

Comparison of Force-Displacement relationship for 1m long, 100mm diameter polyethylene pipe

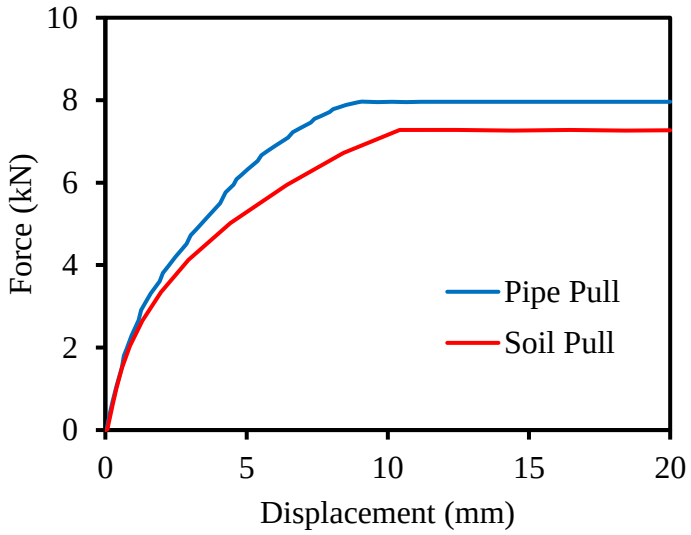

Comparison of Force-Displacement relationship for 6.5m long, 100mm diameter polyethylene pipe

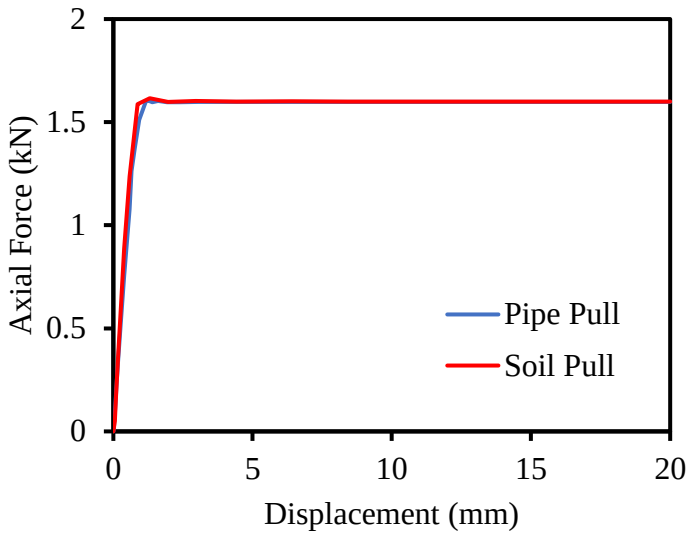

Comparison of Force-Displacement relationship for 1m long, 60mm diameter polyethylene pipe buried at a depth of 600mm

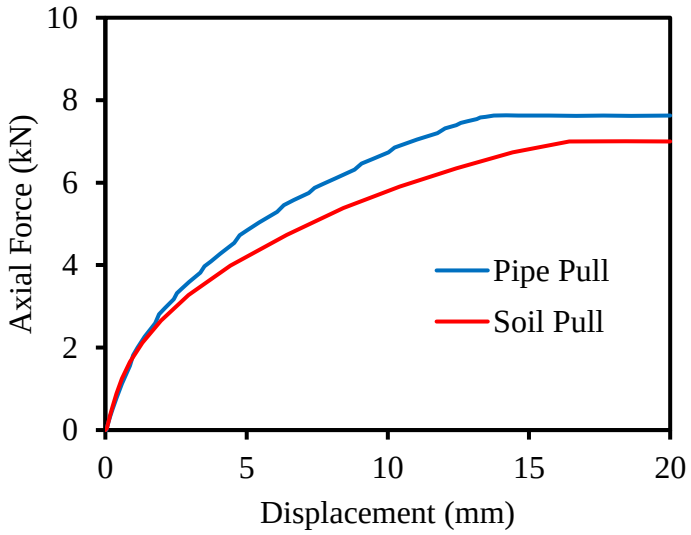

Comparison of Force-Displacement relationship for a 6.5m long, 60mm diameter polyethylene pipe buried at a depth of 600mm

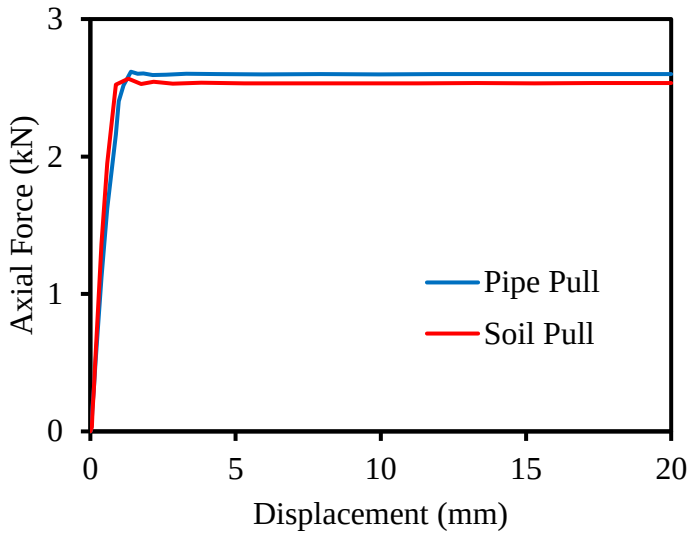

Comparison of Force-Displacement relationship for 1m long, 100mm diameter polyethylene pipe buried at a depth of 600mm

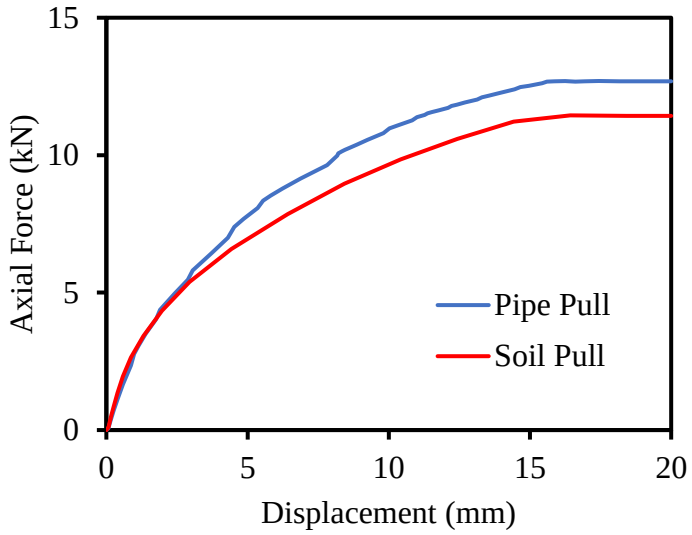

Comparison of Force-Displacement relationship for 6.5m long, 100mm diameter polyethylene pipe buried at a depth of 600mm